Sulfide Oxidation Mechanisms: Controls and Rates of Oxygen Transport

A.I.M. Ritchie

Environmental Science

Australian Nuclear Science and Technology Organisation

PMB 1, Menai, NSW 2234 Australia

8.1. INTRODUCTION

The oxidation of pyrite is common to the processes of metal extraction in leach heaps, to pre-treatment of refractory gold ores in biooxidation heaps, to the pre-treatment of gold ores in biooxidation tanks, and to pollutant generation from pyritic wastes. In the first three cases there is a desire for economic reasons to achieve high oxidation rates. For this reason there has been a major thrust over the last thirty years or so to maximize pyrite oxidation rates. It must be appreciated, however, that an oxidation consumption rate of 10^{-9} kg m^{-3} s^{-1} in a dump of pyritic material 25 ha in area and 15 m high can produce about 4 t of copper a year if the sulfate copper ratio in drainage from the dump is 50:1. This oxidation rate is 10^3 to 10^4 times lower than the rates sought in mineral treatment, but is still high enough to be environmentally significant. This means that, although some of the mechanisms and concepts are common to both the mineral extraction and environmental situations, some are not. In common to both is the pivotal role of the oxygen supply rate to oxidation sites. It is easy to show that, even at the low oxidation rates that are environmentally significant, the oxygen supply rate can restrict oxidation to a comparatively small region of the pyritic wastes. This has an impact on the time dependence of the pollution load from pyritic wastes, as well as on the magnitude of the load.

The second section of this Chapter contains an overview of the processes of pollutant generation in pyritic wastes, and of the role that oxygen supply plays in controlling the overall oxidation rate within the wastes. A picture is presented of the space dependence of pollutant generation in pyritic wastes and how the picture evolves with time. The emphasis is on waste rock rather than tailings because more oxygen supply mechanisms come into play in waste rock than in tailings. The overview is followed by a more detailed examination of oxygen transport mechanisms in porous

material, and on the set of equations that can be used to quantify the overall oxidation rate in a mass of pyritic material. Of importance here is the non-linear interaction between pyrite oxidation rate and gas, water, and heat transport.

Some simple models of the intrinsic oxidation rate (see Section 8.2.4 for a definition) are presented in Section 8.5, together with the overall oxidation rate and pollutant levels to be expected with each of these models. The attraction of these simple models is that they possess important features of actual intrinsic oxidation rates, and they indicate the impact that the intrinsic oxidation rate has on the time dependence of the overall oxidation rate in a waste-rock dump. They provide a quick, quantitative assessment of the pollutant load that might be expected from a waste-rock dump, and also provide some insight to those features of an actual intrinsic oxidation rate which have an impact on the performance of a waste-rock dump. The last section contains a discussion on how the intrinsic oxidation rate of material in pyritic wastes can be measured. Also presented are some data on intrinsic oxidation rates that have been obtained from such measurements on waste dumps.

8.2. POLLUTANT GENERATION AND TRANSPORT

8.2.1. Overview of the Geochemistry of Pyrite Oxidation

a. Pyrite Oxidation

The equations used to describe the oxidation of pyrite are given in Figure 8.1. Below about pH 3 the oxidation of pyrite by ferric ion (reaction 3 of Figure 8.1) is about ten to a hundred times faster than by oxygen (reaction 1 of Figure 8.1) where there is only a small dependence of rate on pH (Moses *et al.*, 1987). Under abiotic conditions the rate of oxidation of pyrite by ferric ion is controlled by the rate of oxidation of ferrous ion (reaction 2 of Figure 8.1), which decreases rapidly with

1. $FeS_2 + {}^7/_2 O_2 + H_2O \rightarrow FeSO_4 + H_2SO_4,$ $\Delta H = 1440 \text{ kJmol}^{-1}$

2. $2FeSO_4 + H_2SO_4 + {}^1/_2 O_2 \rightarrow Fe_2(SO_4)_3 + H_2O,$ $\Delta H = 102 \text{ kJmol}^{-1}$

3. $FeS_2 + Fe_2(SO_4)_3 + 2H_2O + 3O_2 \rightarrow 3FeSO_4 + 2H_2SO_4$

4. $MS + Fe_2(SO_4)_3 + {}^3/_2 O_2 + H_2O \rightarrow MSO_4 + 2FeSO_4 + H_2SO_4$
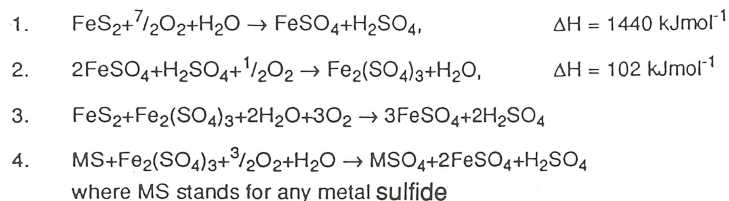   where MS stands for any metal sulfide

Figure 8.1.   Equations of sulfide oxidation.

decreasing pH. Certain bacteria, principally *Thiobacillus ferrooxidans*, catalyze the oxidation of ferrous ion and increase the rate of this reaction by a large factor which has been estimated at about 10^5 (Singer and Stumm, 1970). Although this factor is commonly quoted in discussing the importance of microbial ecology in ARD, in practice the rate of pyrite oxidation under biotic conditions is about ten to a hundred times faster than the abiotic chemical rate (Olson, 1991). Reaction 1 is also catalyzed by bacteria, and it follows that the pH dependence of the oxidation rate in waste-rock dumps may well be overstated.

1. Calcite:
    $CaCO_3 + H_2SO_4 \rightarrow CaSO_4 + H_2O + CO_2$

2. Dolomite:
    $CaMg(CO_3)_2 + 2H_2SO_4 \rightarrow CaSO_4 + MgSO_4 + 2H_2O + 2CO_2$
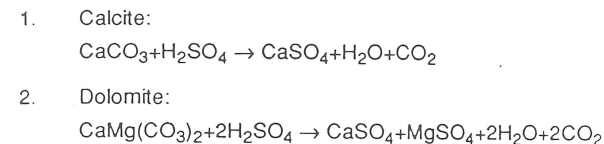
Figure 8.2.   Equations of the dissolution of carbonate by acid.

Reaction 4 in Figure 8.1 is a general description of the oxidation of other metal sulfides present with pyrite in the waste-dump material. Reaction 1, which is just the sum of reactions 2 and 3, is useful in estimating both the quantities of water and oxygen required to fuel the oxidation of pyrite in waste-rock dumps, and the quantity of heat generated.

It should be stressed that the equations in Figure 8.1 do not describe all of the mechanisms involved in the oxidation of pyrite which, from a chemical and microbiological point of view, is a complex of a set of complex reactions. For example, it has been shown that under both abiotic (Reedy *et al.*, 1991) and biotic conditions (Gould *et al.*, 1989), the majority of oxygen atoms in the sulfate is derived from the water. Thus, although the presence of oxygen or ferric ion is essential as the primary oxidant, water plays a pivotal role in the oxidation process. This role is obscured in equations 1 to 3, which describe the net or overall process.

In the same vein, it has been reported (Pronk *et al.*, 1992) that *Thiobacillus ferrooxidans* can grow under anaerobic conditions by using ferric ion as the terminal electron acceptor. Again the implication is that bacterially catalyzed oxidation of sulfide can proceed in a waste-rock dump even when oxygen is expended. In practice, there needs to be a source of ferric ion. A continuing source requires oxygen as described by reaction 2 in Figure 8.1. Alternatively, the ferric ion can be present in a 'rehabilitated' waste-rock dump as a result of oxidation conditions prior to rehabilitation. In practice, the mechanism allows a small spatial extension of the oxidation region (to be described below), or a relatively short-term extension of pyrite oxidation until the ferric-ion inventory is depleted.
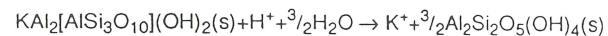
b. Carbonate Dissolution

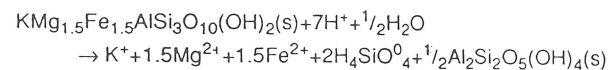Carbonate is generally present in waste-rock dump material, usually as calcite,

but sometimes as dolomite. The reactions describing the dissolution of carbonate by acid produced in pyritic oxidation are presented in Figure 8.2. Again, these do not describe the actual mechanism but do indicate the overall reactions from which it is possible to evaluate stoichiometric relations.

An important property of carbonate dissolution is that it is relatively fast compared to the rate of other mechanisms that control pyrite oxidation in waste-rock dumps. A further important property is that carbonate buffers the pH of pore water in the waste-rock dump at a pH near neutral. An important consequence is that, because chemical species containing many of the trace metals which are important pollutants in ARD are not soluble at pH values much above 4.5, trace-metal pollution is absent while the buffering action of carbonate persists. If there is a large fraction of calcite in the dump material, the concentration of gypsum in pore water may rise to a level at which gypsum precipitates. This level is about 600 mg L^{-1} of Ca, and 1300 mg L^{-1} sulfate, depending on the detailed chemical conditions of the pore water. The precipitation of gypsum is part of the formation of "hardpan" layers found in tailings dams (Boorman and Watson, 1976; Blowes *et al.*, 1991). Although this is a noteworthy process in tailings dams and may present a means of "capping" tailings dams in the long term, hardpan formation is less likely in the much coarser material comprising a waste-rock dump.
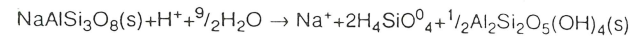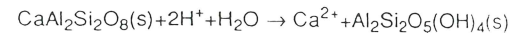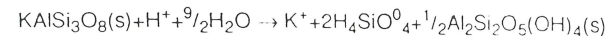
c. Gangue Dissolution

Several reactions describing the dissolution of some of the more common gangue materials are presented in Figure 8.3. These reactions have been chosen in part because the minerals are typical constituents of rock, and partly because the reaction rates are slow and likely to be important in the long-term evolution of the chemical composition of pore water in a waste-rock dump. These reactions are responsible for the concentrations of major ions such as Cu, Mg, Na, K, Al, and sulfate in the drainage water. The pH of the pore water depends on the presence of various mineral species and on the rates of reaction. In general, the pH in the drainage water decreases with time as various reactions proceed within the waste-rock dump until pH reaches the 2.0—4.0 range characteristic of ARD. Even if the pH of the drainage from a waste-rock dump remains sufficiently high that trace-metal concentrations are too low to be of environmental significance and the drainage does not have the 'classical' characteristic of ARD, the total dissolved salt (TDS) concentration could be too high to be environmentally acceptable.

1. Muscovite dissolution:
   $$KAl_2[AlSi_3O_{10}](OH)_2(s)+H^++{}^3/_2H_2O \rightarrow K^++{}^3/_2Al_2Si_2O_5(OH)_4(s)$$

2. Biotite dissolution:
   $$KMg_{1.5}Fe_{1.5}AlSi_3O_{10}(OH)_2(s)+7H^++{}^1/_2H_2O$$
   $$\rightarrow K^++1.5Mg^{2+}+1.5Fe^{2+}+2H_4SiO^0_4+{}^1/_2Al_2Si_2O_5(OH)_4(s)$$

3. Albite dissolution:
   $$NaAlSi_3O_8(s)+H^++{}^9/_2H_2O \rightarrow Na^++2H_4SiO^0_4+{}^1/_2Al_2Si_2O_5(OH)_4(s)$$

4. Anorthite dissolution:
   $$CaAl_2Si_2O_8(s)+2H^++H_2O \rightarrow Ca^{2+}+Al_2Si_2O_5(OH)_4(s)$$

5. K-feldspar dissolution:
   $$KAlSi_3O_8(s)+H^++{}^9/_2H_2O \rightarrow K^++2H_4SiO^0_4+{}^1/_2Al_2Si_2O_5(OH)_4(s)$$

6. Iron precipitation:
   $$Fe^{3+}+3H_2O \rightarrow Fe(OH)_3(s)+3H^+$$
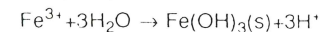
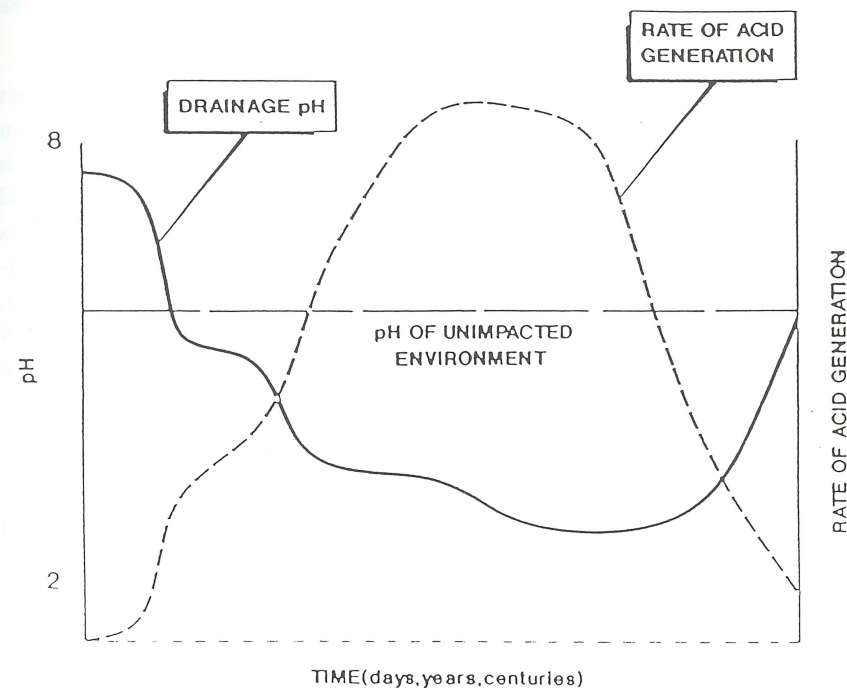Figure 8.3.   Equations of typical gangue-dissolution reactions.

Figure 8.4.   Schematic diagram of the evolution of acid drainage (adapted from B.C. AMD Task Force, 1989).

8.2.2. Evolution of ARD

Figure 8.4 shows a schematic diagram of the evolution of acid drainage on the basis of U.S. and Canadian studies as reviewed by the British Columbia AMD Task Force (1989). In this picture the slow initial rate corresponds to the "slow" rate of reaction 1 in Figure 8.1, which is the dominant reaction at high pH. As pyrite oxidation proceeds, the pH decreases in a series of steps, each of which represents the dissolution of a specific buffering species present at that pH (Morin *et al.*, 1988a,b; Morin and Cherry, 1988; Morin, 1988). The mineral species believed responsible for each of the pH plateaux are

- calcium-based carbonate pH 5.5 to 6.4
- aluminum hydroxide pH 4.3 to 5.0
- iron hydroxide and jarosites pH 3.0 to 3.7

With decreasing pH the oxidation rate is thought to increase as both the increasing bacterial population and the increasing effect of reactions 2 and 3 of Figure 8.1 come into play. At some stage the pyrite oxidation rate reaches a maximum, thereafter decreasing as the quantity of readily oxidizable pyrite decreases. Eventually all of the available pyrite is oxidized, and drainage returns to a near-neutral pH.

It should be noted that Figure 8.4 has no numerical scale on the pyrite oxidation rate. This absence largely reflects the small amount of data currently available on oxidation rates within waste-rock dumps. It should also be noted that the description infers that the whole waste-rock dump is acting as a well-stirred chemical reactor, and that largely chemical-based reaction rates dominate the pollution-generation process within a waste-rock dump. It will be shown below that, in reality, the pollutant-generation process in a waste-rock dump is expected to be strongly space-dependent, that the description of a waste-rock dump as a single well-stirred chemical reactor is inappropriate in all but some special cases, and that the dominant rate controls are not chemical or biological.

8.2.3. Rates of Reactions

Table 8.1 is a comparison of pyrite oxidation rates derived from: a set of laboratory experiments with the focus on microbiological mechanisms, a set of laboratory experiments with the focus on chemical mechanisms, and measurements in a waste-rock dump in which oxidation is occurring. The oxidation rates derived from the first two sets of experiments can readily be compared with each other, but there are some reservations in making a direct comparison of results of the first two sets with the third set. The third set results from measurements in a waste-rock dump in which pyrite oxidation is the dominant oxygen-consumption process, and the results represent an

Table 8.1. Comparison of oxygen consumption rates derived from different types of experiment

Type of experiment	Conditions of experiment	Quoted rate	Normalized rate (kg m^{-3} s^{-1} at a dump pyrite density of 56.3 kg m^{-3})	Reference
Microbiological mechanism	Comparison of results from 8 labs; 1 g pyrite in 50 mL pH 3—3.4, 28 °C	(mg Fe L^{-1} h^{-1}) range 7.8—17.8 average 12.4 abiotic rate average 0.36	1.9x10^{-5} from biotic average 5.6x10^{-7} from abiotic average	Olson (1991)
Chemical mechanisms	Oxidation in D.O. saturated solutions and ferric solutions; the data quoted are for D.O. solutions, pH 2.2— 9.1, 22—25 °C; results normalized to 1 g pyrite in 300 mL	(mmol min^{-1} SO$_4$) range 0.021—0.085 average 0.057	3.2x10^{-6} from average rate	Moses et al. (1987)
Measurements in waste-rock dumps	Inferred from temperature profiles measured in a dump pH 2.0—4.0, 35—56 °C	(kg m^{-3} s^{-1}) range 0.3—8.8x10^{-8}	1.0x10^{-8} for model dump	Harries & Ritchie (1981)

Table 8.2. Comparison of chemical kinetic rates for waste-rock minerals

Process	Description	Reaction rate per unit surface area of mineral (mol m^{-2} s^{-1})
1, Fig. 8.1	pyrite oxidation	5.12 x 10^{-8}
1, Fig. 8.3	muscovite dissolution	6.32 x 10^{-12}
2, Fig. 8.3	biotite dissolution	2.57 x 10^{-9}

oxygen-consumption rate integrated over a large volume. The fact that the third set is from such an integral measurement is one of the points of the comparison. It shows that, in a waste-rock dump which is posing an environmental problem, the oxygen-consumption rates are low and are much lower than might be expected on the basis of laboratory experiments. This is not to say that rates in all heaps of pyritic material are low. If this were so, then the overall oxidation rates sought in biooxidation heaps would be unattainable. Rather, the point is to emphasize that oxygen-consumption rates in a waste-rock dump can be orders of magnitude lower than rates of pyrite oxidation measured in the laboratory and, as will be shown below, the rates have an impact on the space and time dependence of pollutant production in the dump and on the time dependence of polluted drainage from the dump.

In comparison with the slow rate of acid generation in a waste-rock dump, it is reasonable to assume that acid neutralization by acid-consuming materials such as

carbonates will be fast enough to react with acid close to the point of production in the dump, and that this acid neutralization will continue until all such fast-reacting, acid-consuming materials are used up. After that, acid will be transported by water from the point of production to parts of the dump below the point of production. In comparison with carbonate-dissolution rates, most other gangue-dissolution rates are slow. It is beyond the scope of this paper to discuss these rates at length. Table 8.2, however, compares pyrite-oxidation kinetic data (see Nicholson, this Volume) with the kinetic data for the dissolution of the two gangue minerals listed in Figure 8.3. It can be seen that, provided that integration over the surficial mineral-surface area does not greatly affect the relative rates, the rates of these reactions are substantially lower than pyrite oxidation rates.

Table 8.3. Physical properties of a dump of mine waste

Symbol	Definition	Value	Units
L	Dump height	15	m
A	Dump area	25	ha
ρ_r	Bulk density of dump material	1500	$kg\,m^{-3}$
ρ_{rrs}	Sulfur density as pyrite	30 (2%)	$kg\,m^{-3}$
Q_w	Infiltration rate	0.5	$m\,y^{-1}$
ε_g	Gas-filled porosity of the dump material	0.30	
ε_w	Water-filled porosity at specified infiltration	0.10	
K_s	Saturated hydraulic conductivity of the dump	10	$m\,d^{-1}$
D	Oxygen diffusion coefficient in the dump	5.0×10^{-6}	$m^2\,s^{-1}$
C_o	Oxygen concentration in air	0.265	$kg\,m^{-3}$
ε	Mass of oxygen consumed per unit mass of sulfur oxidized	1.75	

Table 8.4. Masses of oxygen and water required to oxidize the pyrite in the dump

Mass of oxygen required to oxidize pyrite	200,000 t
Mass of oxygen initially in the pore space of the dump	300 t
Mass of water required to oxidize pyrite	32,000 t
Mass of water initially in the pore space of the dump	375,000 t

8.2.4. Rate Controls

In discussing mechanisms that control pollutant-generation rates in pyritic waste-rock dumps, it is helpful to have a specific waste dump in mind. Such a dump, with parameters typical of a waste-rock dump, is specified in Table 8.3. The masses of oxygen and water required to oxidize all of the pyrite in the dump are given in Table 8.4. It is clear that, whereas the water inventory in the dump is some ten times greater than the amount required to oxidize the pyrite, the initial oxygen inventory is about a thousand times too small. It follows that oxygen has to be supplied to support pyrite oxidation in the dump whereas, on the basis of the stoichiometry of pyrite oxidation, water does not.

There are three mechanisms that transport oxygen from the outer surfaces of a dump to oxidation sites within the dump:

- dissolved in infiltrating rainwater

- diffusive transport through the gas-filled pore space

- advective transport through the gas-filled pore space

As discussed in more detail in Section 4 below, the first mechanism is of negligible significance in most circumstances. Diffusion is a common and significant transport mechanism in waste-rock dumps, and advection in the form of convection has been identified as a gas transport mechanism in waste-rock dumps (Harries and Ritchie, 1985; Lefebvre *et al.*, 1992). It is reasonable to expect that advection driven by pressure gradients consequent on wind-driven airflow over waste-rock dumps would also be a gas transport mechanism, but such an effect has not been quantitatively identified.

Several authors have included gas transport in modelling pyrite oxidation in dumps of pyritic material (Cathles and Schlitt, 1980; Jaynes *et al.*, 1984; Davis and Ritchie, 1986, 1987; Davis *et al.*, 1986; Pantelis and Ritchie, 1991a,b, 1992, 1993). Pantelis and Ritchie used the expression "intrinsic oxidation rate" for the term in the pore oxygen-transport equation that describes the loss of oxygen from the dump pore space by oxidation reactions in the material comprising the dump. It has been shown that, unless the intrinsic oxidation rate of the dump material is low, it is the oxygen transport rates that control the rate at which pyrite oxidizes in a dump. It has further been shown by Pantelis and Ritchie (1991a) that convection is rapidly established in a dump with an air permeability of 10^{-9} m^2 or higher, but diffusion dominates in a dump with an air permeability of 10^{-10} m^2. The air permeability in waste-rock dumps is generally in the range 10^{-12}—10^{-9} m^2 (J.W. Bennett 1993, private communication). Moreover, as convection is established first in the toe of a dump and propagates from there into the main body of a dump (Pantelis and Ritchie, 1992), diffusive transport tends to be the dominant gas transport mechanism in large waste-rock dumps. The interaction of diffusion, convection, and the intrinsic oxidation rate in determining the overall oxidation rate is discussed in more detail in Section 5 below.

It also follows that, in a dump in which diffusive transport dominates, oxidation is confined to a region that starts at the outer surfaces of the dump and propagates inward. The spatial extent of this region depends on the ratio of the intrinsic oxidation rate to the oxygen diffusion coefficient; the larger the ratio the smaller the region until,

at large intrinsic oxidation rates, oxidation in the dump conforms to the simple homogeneous model discussed by Davis and Ritchie (1986) and in Section 5.2 below.

8.2.5. *Space and Time Dependence of Pollutant Generation*

Figure 8.5 is a schematic diagram of the space dependence of pyrite oxidation and associated chemical reactions in a waste dump in which gas transport is by both diffusion and convection. As shown, there are three distinct regions.
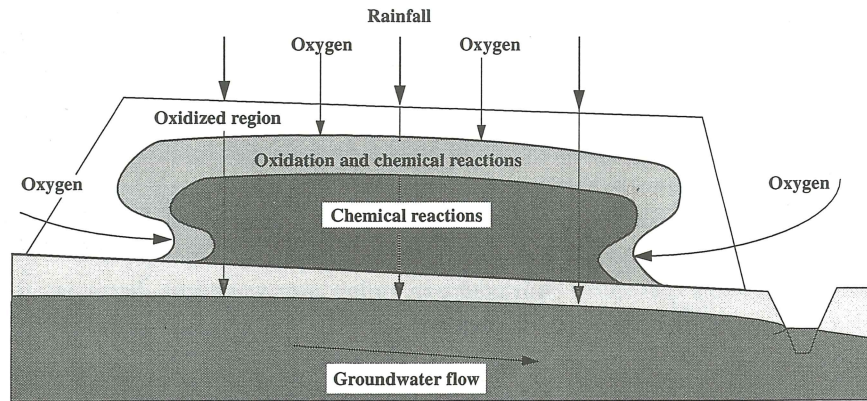
Figure 8.5.   Schematic representation of pollutant generation and transport processes in a pyritic waste-rock dump.
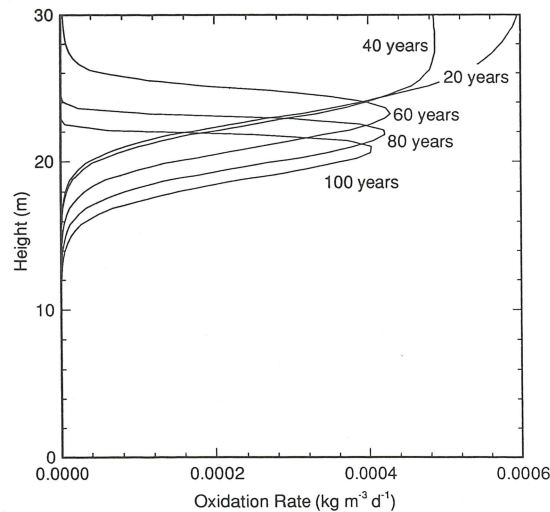
Figure 8.6.   Oxidation rates as a function of depth for an uncovered dump at 20-year intervals. The parameters are given in Table 8.6.

In the outer region, all of the oxidizable material has been oxidized. This region is non-reactive from an ARD viewpoint, with no absorption of oxygen and no chemical reactions. In the second region, pyrite is oxidizing and the oxidation products interact with other constituents of the dump material. The lower boundary of this region is defined by the point where the oxygen concentration falls to zero. In the inner region, the only products of pyrite oxidation are those transported down by water infiltrating the dump. If the intrinsic oxidation rate is very low, then the second region can encompass the whole of the waste-rock dump.

The pH of the second region remains high as long as the buffering action of carbonate persists. The timescale for this depends primarily on the magnitude of the intrinsic oxidation rate and the amount of carbonate in the material of the waste-rock dump; the scale can be of the order of years. Thereafter, a pH front propagates down through the inner region at a rate that depends primarily on the acid production rate in the oxidation region, the carbonate concentration in the dump, and on the specific discharge rate of water through the dump. This pH front eventually reaches the base of the dump. Further pH fronts propagate through the dump until the pH at the base of the dump corresponds to a pH at which trace metals are soluble. At this stage, drainage at the base of the dump assumes the characteristics of ARD. It is frequently at this stage that the mine operator realizes that an ARD problem exists. This can be many years after initial construction of the waste-rock dump.

In a dump in which ARD is well-established, there will be a decrease in pH from the top of the second region to its base. In the inner region there will be a pH gradient and a gradient in other chemical species in the pore water from the top of the inner region to the base of the dump. The details of the gradients in the inner region depend on the detailed mineral composition of the dump. It should be noted, however, that the boundaries of the second region typically move sufficiently slowly that pseudo-steady-state conditions can be assumed in chemical modelling of most dumps.

It should be noted that the effluent from the toe of a waste-rock dump is not a direct measure of drainage from the base of the dump. Rather, it is some integral of drainage from a large area of the base; the time dependence of the chemical composition of effluent at the toe is some convolution of the transit times from points at the base of the dump which contribute to drainage at the particular part of the toe where the effluent is sampled. Thus, the chemical composition of such effluent provides only a limited amount of information on pollutant-generation rates within the dump. The fact that effluent from such a point is an integral of drainage from some portion of the waste-rock dump does provide access to some integral properties of pollutant generation if the flow rates, as well as pollutant concentrations, are monitored. It is unfortunate that at many minesites there is a wealth of data on the chemical composition of ARD, but data on flow rates are sparse at best.

Table 8.5: Typical timescales associated with pyritic oxidation in a dump of mine waste

	Intrinsic oxidation rate (kg of oxygen m^{-3} s^{-1})		
	low, 1 x 10^{-8}	medium, 10 x 10^{-8}	high, 100 x 10^{-8}
Time to use up the initial pore-space oxygen	92 d	9.2 d	0.92 d
Time to oxidize all pyrite	166 y	150 y	142 y
Time to oxidize all of the pyrite if the intrinsic oxidation rate is infinitely high		142 y	
Time to completely oxidize a particle 4 mm in diameter assuming a shrinking-core model		66 d	
Time for bacterial population to increase by a factor of one million		about 20 d	
Time for flow at base to respond to an increased infiltration rate at the surface		about 1 d	
Transit time for water from top to base of dump if whole depth is unsaturated		about 3 y	
Transit time for water to pass along the length of the base if the base is saturated		about 5 y	

It is instructive in understanding the dynamics of pollutant production, pollutant transport, and ARD to compare the timescales of the various processes. Some of these are presented in Table 8.5 for the waste-rock dump specified by the data in Table 8.3. The timescale to consume all of the pyrite in the dump is based on the assumption that diffusion is the dominant gas transport mechanism. It should be noted that, at the low oxidation rate of Table 8.5, region two, the region where oxidation and chemical reactions occur, encompasses the whole dump. At the higher rates, oxidation moves through the dump with a $t^{1/2}$ time dependence after an initial transient. It follows that, if the dump were 30 m high rather than 15 m high, the time to oxidize all of the pyrite would increase from about 150 years to 600 years.

These timescales mean that the short-term (days to years) time dependence of the quantity and quality of drainage from the base of a waste-rock dump depends on the height of the dump, water transport mechanisms in the dump, the rate of water infiltration into the top surface of the dump, where and at what rate pyrite oxidation proceeds in the dump, and the concentration of fast-reacting, acid-consuming materials such as carbonates. The long-term (years to tens to hundreds of years) time dependence depends on the relative magnitude of the gas diffusion coefficient and the intrinsic oxidation rate, and on the dissolution rate of gangue minerals. It is also clear that when the ratio of the intrinsic oxidation rate to the diffusion coefficient is high, then the intrinsic oxidation rate is in effect infinitely large and does not need to be known with any precision. This point is quantified in Section 5 below.

Some of the above points are illustrated in Figures 8.6, 8.7 and 8.8, which show results from computer simulations of the effectiveness of different cover systems on a
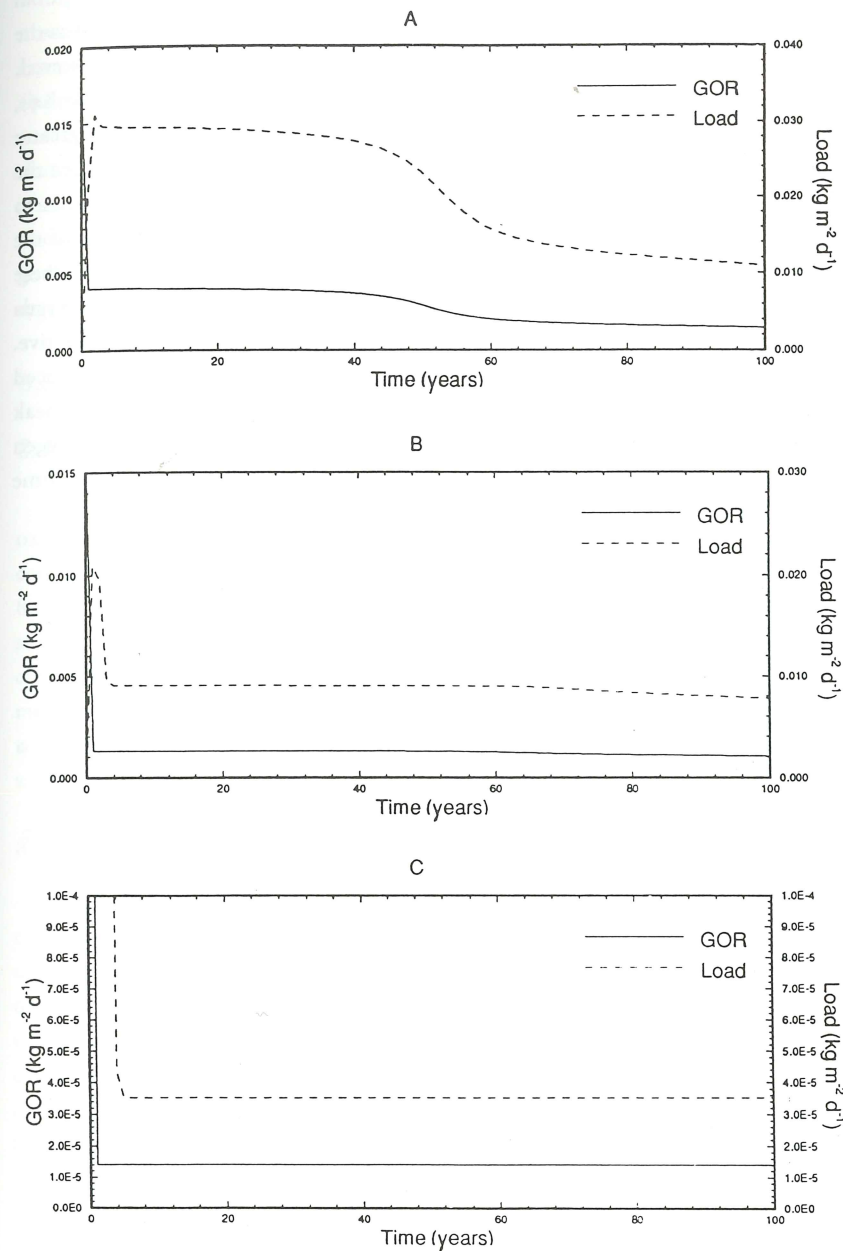

Figure 8.7.   The overall oxidation rate (GOR) and sulfate load at dump base as a function of time for three cases. The parameters are given in Table 8.6; (a) uncovered dump; (b) 0.5 m cover, Ks = 0.01 m/d: (c) 1.0 m cover, Ks = 0.001 m/d.

waste-rock dump, using the parameter values presented in Table 8.6. The global oxidation rate is the space-integrated oxidation rate in the dump, and the load is the sulfate load in drainage from the base of the dump, assuming that sulfate is conserved. Figure 8.6 indicates that, even at the low intrinsic oxidation rate used (see Table 8.6), the oxidation rate is confined to a relatively small region of the dump at times greater than about 60 years. Figure 8.7 shows that the effect of the covers, which reduce the oxygen flux into the dump but which do not alter the water infiltration rate, is to reduce the global oxidation rate and the load at early times. The effectiveness of the cover with $K_s = 0.01$ m d^{-1} at times greater than about 60 years is not great; at these times the oxidized upper layer is just as effective as the cover in reducing the oxygen flux. Figure 8.8 demonstrates just why the cover with $K_s = 0.001$ m d^{-1} is so effective. The oxidation rate, and hence the pollution-production rate, are greatly reduced because this cover greatly reduces the oxygen flux into the dump. The short-lived peak in the load at early times in Figure 8.6 is just oxidation from the initial oxygen inventory of the dump. For this reason it is unaffected by the covers. The time dependence of this peak reflects water transit times in the dump.
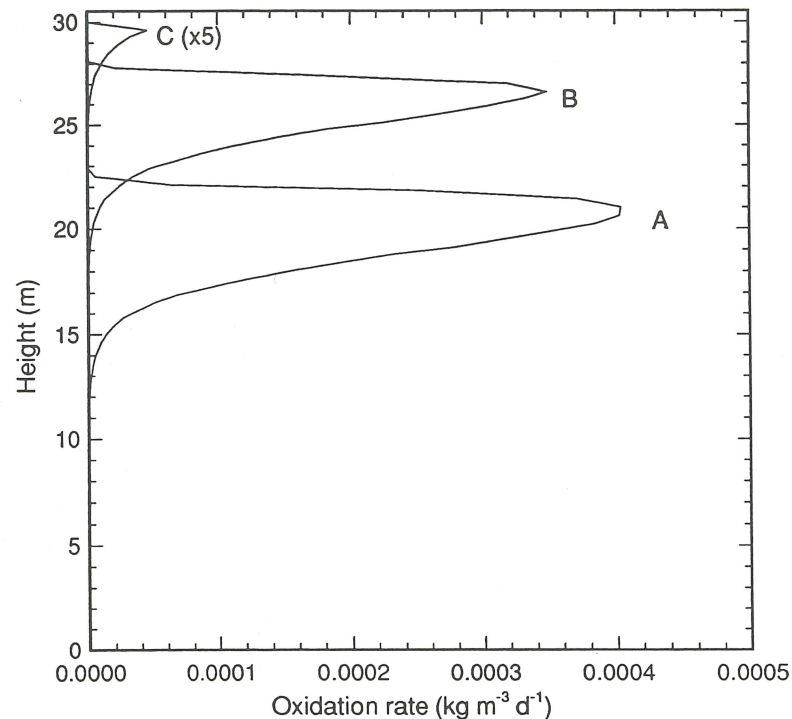

Figure 8.8.   Oxidation rate after 100 years as a function of depth for three cases. The parameters are given in Table 8.6; (a) uncovered dump; (b) 0.5 m cover, Ks = 0.01 m/d; (c) 1.0 m cover, Ks = 0.001 m/d.

The schematic representation of the space dependence of pollutant generation in a waste-rock dump (Figure 8.5) assumes homogeneity of the dump material, and the same concept can be applied where the dump is not homogeneous. Given that the appropriate scale for the transport processes important in defining the overall oxidation rate in pyritic wastes is a meter or so, and that the bulk physical properties that determine the magnitude of the transport rates appear not to vary appreciably over a scale of tens of meters (see Chapter 5), it is practical and appropriate to consider a dump as a set of contiguous, homogeneous dumps. This is particularly so when the goal is to assess the effectiveness of rehabilitation strategies rather than to explain detailed variability from one part of a dump to another.

8.3. OXYGEN TRANSPORT MECHANISMS

8.3.1. Oxygen Dissolved in Rainwater

Oxygen dissolved in rainwater infiltrating a waste-rock dump is a source of oxygen for pyrite oxidation within the dump. At 25 °C the saturated dissolved-oxygen concentration in water is about 8 mg/L. At the rainfall infiltration rate given in Table 8.3 the corresponding oxygen flux is 1.3×10^{-10} kg m^{-2} s^{-1}. If this is converted to sulfate according to the stoichiometry of reaction 1 in Figure 8.1, and if sulfate is conserved in the dump, this oxygen flux supports a sulfate concentration of about 14 mg/L. This is very much lower than the sulfate concentrations usually associated with acid rock drainage and indicates that, in the context of acid rock drainage, oxygen-saturated rainwater is not a significant oxygen supply mechanism.

8.3.2. Diffusion Through the Dump Pore Space

Oxygen removed from the dump pore space by pyrite oxidation sets up a concentration gradient in the pore space. Although such gas removal will initially set up a pressure gradient, the gradient is rapidly removed by mass transport of air into the dump. The transport mechanism is then by diffusion of oxygen into the dump in primarily an oxygen — nitrogen gas mixture, and by nitrogen diffusion out of the dump. To estimate the pyrite oxidation rate that can be supported by such a mechanism, it is simplest to assume that the intrinsic oxidation rate is very high. It is then easy to show (see Section 5 below) that the oxidation rate of the sulfidic sulfur is:

$$G(x^*, t^*) = \delta(x^* - x^*(t^*)) \sqrt{\frac{(DC_o \varepsilon \rho_{rs})}{(2t^*)}} \qquad (1)$$

$$X^*(t^*) = \sqrt{\frac{(2DC_o t^*)}{(\varepsilon \rho_{rs})}} \qquad (2)$$

With the dump parameters given in Table 8.3, and again assuming conservation of

sulfate, the sulfate concentration in pore water percolating a 5-year-old dump is 45.8 g/L. The corresponding oxygen flux into the dump at the surface is 4.3×10^{-7} kg m^2 s^1. These quantities indicate that gas diffusion can support oxidation rates at environmentally significant levels. Oxygen concentration profiles that can be ascribed to diffusive gas transport have been observed both in waste-rock dumps and in tailings dams (Harries and Ritchie, 1985; Lefebvre *et al.*, 1992; Blowes *et al.*, 1991).

8.3.3. Convection

Because pyrite oxidation is very exothermic (see reaction 1 in Figure 8.1), and as soil is generally a poor conductor of heat, relatively modest oxidation rates give rise to elevated temperatures in waste-rock dumps. Temperatures of 50—60 °C are not uncommon (Harries and Ritchie, 1981; Lefebvre *et al.*, 1992). The resulting temperature gradients give rise to in-dump density gradients that lead to convective transport of gas and to the rapid replacement of oxygen, consumed in the dump, by air moving in from the surface of the dump. Gas specific-discharge rates are about 5×10^{-5} m s^{-1} at a temperature rise in a dump of about 50—60 °C and an air permeability of 10^{-9} m^2. At an oxygen density of 0.265 kg m^{-3} in air, the oxygen flux at the dump surface caused by this convective gas flow is 1.3×10^{-5} kg m^{-2} s^{-1}. Although this is a substantially higher flux than the diffusive flux quoted in Section 3.2 above, the convective flux in a large dump generally applies over a much smaller area than does the diffusive flux. It does, however, indicate that convection can be a significant oxygen-supply mechanism. Oxygen concentration profiles which can be ascribed to convective transport have been observed in a number of waste-rock dumps (Harries and Ritchie, 1981; Lefebvre *et al.*, 1992).

8.3.4. Advection

Many waste-rock dumps are constructed on comparatively flat areas. Wind blowing over the dump generates pressure differences in much the same way as those over an aircraft wing. Assuming a wind velocity of 10 ms^{-1} (36 km h^{-1}) and the dump properties of Table 8.3, simple fluid-flow considerations indicate a pressure gradient of about 1 Pa m^{-1} in the region of the dump batters. At an air permeability of 10^{-9} m^2, the gas specific-discharge rates are then about 2×10^{-5} ms^{-1}. This is of the same order as those generated by temperature gradients, and it is therefore reasonable to expect advective gas transport in waste-rock dumps. Such an effect has not been quantitatively identified. A possible reason is that, whereas a temperature gradient in a waste-rock dump persists on a timescale of years, the persistence timescale for wind velocities is more like hours. Because the transit time for gas through a dump under these wind-induced pressure gradients is a few hours or more, this form of advective transport may not last long enough to support a significant oxidation rate.

Table 8.6. The values of the parameters used in computer simulations of cover systems

Quanity	Definition	Value
Q_w	Irrigation rate (md^{-1})	1.5×10^{-3}
L	Height of dump (m)	30
D	Cover layer thickness (m)	case dependent
K_{sw}	Saturated hydraulic conductivity, waste rock (m d^{-1})	10
K_{sc}	Saturated hydraulic conductivity, cover (md^{-1})	case dependent
α	Capilary parameter (m^{-1})	= 3.0 (waste material) = 1.0 (cover layer)
ε_s	Volume fraction of dump material (= 1-porosity)	0.6
ρ_s	Bulk density of dump material (kg m^{-3})	1500
S_{max}	Maximum intrinsic oxidation rate (kg (O$_2$) m^{-3}s^{-1})	2×10^{-8}
ρ_{rs}	Sulfur density as pyrite (kg m^{-3})	15

Oxygen Mass Fraction

$$\frac{\partial(\rho_g \omega^g)}{\partial t^*} + \nabla \cdot [\rho_g \underline{v}^g \omega^g - \rho_g D \nabla \omega^g] = -\varepsilon S_S(\omega^g, \omega^s, T^*)$$

Solid Reactant Mass Fraction

$$\rho_s \frac{d\omega^s}{dt^*} = -S_S(\omega^g, \omega^s, T^*)$$

Heat Equation

$$\Sigma_\alpha \rho_\alpha c_\alpha \frac{\partial T^*}{\partial t^*} + \Sigma_\alpha \rho_\alpha c_\alpha \underline{v}^\alpha \cdot \nabla T^* - \nabla \cdot (K_T \nabla T^*) = \delta S_S(\omega^a, \omega^s, T^*)$$

Macroscopic Pore Velocities

$$\varepsilon_\alpha \underline{v}^\alpha = -\frac{K k_{r\alpha}(\varepsilon_\alpha)}{\mu_\alpha}(\nabla p^\alpha + \rho^\alpha g \hat{z}) \quad \alpha = g, w$$

Mass Balance for the Gas and Water Phases

$$\frac{\partial \rho_\alpha}{\partial t^*} + \nabla \cdot (\rho_\alpha \underline{v}^\alpha) = \sigma^\alpha \quad \alpha = g, w$$

where σ^α is a generic source/sink term. The intrinsic density ρ^α is related to the bulk density ρ_α, by the relationship $\rho_\alpha = \varepsilon_\alpha \rho^\alpha$ ($\alpha = g, w, s$). In the above we must have $\Sigma_\alpha \varepsilon_\alpha = 1$. The water and air intrinsic pressures within the porous medium are related by $p^c(\varepsilon_w) = p^g - p^w$, where $p^c(\varepsilon_w)$ is the capillary pressure which is a function of the water volume fraction ε_w. The intrinsic gas density ρ^g is a function of the gas pressure p^g and the temperature T^*.

Figure 8.9. Equations describing heap oxidation (Pantelis, 1993).

8.4. MATHEMATICAL MODELLING OF GAS TRANSPORT

8.4.1. Model Equations

From the discussion in Section 3, the following physical processes need to be considered in quantifying pyrite oxidation rates in pyritic wastes:

- the pore-gas oxygen concentration

- heat transport in the pyritic waste

- gas transport through the pore space of the wastes

- the intrinsic oxidation rate

Furthermore, because water flow through the wastes transports heat, and because changes in the fraction of pore space filled with water changes the gas-filled volume of pore space (thereby changing such dump properties as the gas diffusion coefficient and air permeability), it is necessary also to model water flow through the waste material.

A set of equations describing the above physical transport processes is given in Figure 8.9. A clear advantage of using this set of equations is that the solution provides not only the pyrite oxidation rate, which is the primary pollution source, but also provides the space and time dependence of the temperature and pore-gas oxygen concentrations within the dump. These are both readily measured quantities. Furthermore, such bulk properties of the waste material as the gas diffusion coefficient, the air permeability, and the thermal conductivity, all of which determine gas transport rates and hence oxidation rates, can all be measured *in situ*. A model based on this set of equations is therefore predictive and does not need to be "calibrated". The question of the variability of bulk properties throughout the dump, and the possible impact of such variation on pollutants loads in drainage, are discussed Chapter 5.

8.4.2. The Intrinsic Oxidation Rate

In principle the intrinsic oxidation rate, which is just the rate at which oxygen is consumed by the dump material, is a function of a large number of variables; these include pore-gas oxygen concentration, particle-size distribution, mineral surface area, bacterial population, temperature, pH, ferric ion concentration, and so on. To include the functional dependence of the intrinsic oxidation rate on these variables means that, for consistency, equations describing their dependence on other variables and on dump properties have to be added to the set of equations in Figure 8.9. This makes even more numerically intensive an already numerically intensive calculation. In practice, and as will be discussed in Section 5 below, the overall oxidation rate in a waste-rock dump is comparatively insensitive to detailed changes in the intrinsic oxidation rate unless the intrinsic oxidation rate is very low. Furthermore, and as is again discussed below, the

characteristic timescales for changes in many of these variables are so much shorter than the timescales of others, that the variables with short timescales will follow, in a time sense, the time dependence of the more slowly changing variables. Variables with small characteristic timescales therefore need not be included as variables in the set of model equations. In addition, as there is a very limited amount of experimental data on the intrinsic oxidation rate of run-of-mine waste rock, it is inappropriate to include more detail than is absolutely necessary in the functional dependence of the intrinsic oxidation rate.

In the same vein it is worth stressing that the purpose of modelling pyrite oxidation in a waste-rock dump is not to predict the conditions at each point of the dump; rather, it is to achieve one or other of the following goals:

- identify mechanisms that are important controls on the overall oxidation rate in the dump, and the sensitivity of the overall oxidation rate to the bulk parameters required to quantify these mechanisms

- assist in planning experimental measurement programs to elucidate gas transport mechanisms

- assess the effectiveness of rehabilitation schemes intended to reduce oxidation rates within a waste-rock dump

- assess the effectiveness of dump construction techniques in reducing oxidation rates

- quantify the pollution loads in drainage, particularly the peak load and the time to peak load

It follows that the intrinsic oxidation rate should be of a form that is physically reasonable and which allows the above goals to be achieved.

There are a number of forms of the intrinsic oxidation rate that satisfy these criteria. Two such are the shrinking-core model (SCM) and a model based on Monod kinetics. These are described below together with a third form with properties close to those of the shrinking-core model.

The shrinking-core model of the intrinsic oxidation rate has the form

$$S\left(\omega^g, \omega^s, T^*\right) = \frac{3\gamma D_2 \varepsilon_s}{a^2} \alpha\left(T^*\right) \rho^g \omega^g \frac{\left(\rho_s \omega^s\right)^{\frac{1}{3}}}{\rho_{rs}^{\frac{1}{3}} - \left(\rho_s \omega^s\right)^{\frac{1}{3}}} \qquad (3)$$

The intrinsic oxidation rate in this form has the following properties:

- it is proportional to the pore-gas oxygen concentration

- it decreases to zero in a smooth fashion as the oxidizable material is consumed

- it decreases increasingly slowly as the oxidizable material is consumed

- it is high at early stages of oxidation of the particles comprising the dump

- small particles oxidize more rapidly than large particles

- it is infinitely fast when oxidation starts on an unoxidized particle

Most of these features are consistent with an intuitive understanding of how sulfidic material oxidizes in pyritic waste. The last feature is the exception. The infinity can be removed by arguing that all the sulfidic material on the surface of a particle is oxidized by the time the waste material is dumped; therefore, the model is started with a thin oxidized layer on the outer rim of each particle.

The temperature dependence $\alpha(T)$ has been included for completeness. Given the large mass of a waste-rock dump, the temperature profile is a slowly varying property of the dump, reflecting the oxidation rate within the dump rather than that imposed by external influences. The ten-folding length for a temperature wave propagating into a dump, with a frequency of the order of that of the annual variation in surface temperature, is typically about 5 m; thus, even with a swing in surface temperature of $\pm 20\ °C$ from summer to winter, the temperature variation 5 m from the surface is only $\pm 2\ °C$. Unless the oxidation process is confined to the near-surface of the wastes, as it commonly is in tailings material, the temperature dependence of the intrinsic oxidation rate can therefore be neglected for most waste-rock dumps. Moreover, as discussed below in Section 6.3, the temperature dependence of run-of-mine waste rock can be much less than expected on the basis of laboratory measurements.

An intrinsic oxidation rate based on Monod kinetics takes the form

$$S\,(\omega^g, \omega^s, T^*) = \varepsilon \rho_g \rho_s \alpha\,(T^*)\sigma_3 \frac{\omega^g}{\sigma_1 + \omega^g} \frac{\omega^s}{\sigma_2 + \omega^s} \qquad (4)$$

With this formulation the intrinsic oxidation rate has the following properties:

- at high values of pyrite and of pore-gas concentration it varies only very slowly with changes in these two variables

- at low values of either the pore-gas oxygen concentration or the pyrite concentration it is effectively proportional to these variables

- the change between the two functional dependencies occurs in a small region of these two variables as defined by the parameters σ_1 and σ_2.

Again, these properties are consistent with those thought applicable to the oxidation of pyrite. It should be noted, however, that with this formulation of the intrinsic oxidation rate neither pyrite nor oxygen is ever completely exhausted. The shrinking-core model, on the other hand, defines an oxidation lifetime for a particle of a given

size so that, with this form of the intrinsic oxidation rate, there a region in the dump where oxidation is complete. In general, this region starts at the dump surface and propagates into the dump as the dump ages. In quantitative terms, the use of expression (4) does in effect lead to an oxidized region, an oxic region, and an anaerobic region as indicated in Figure 8.5.

A much simpler form of the intrinsic oxidation rate that avoids the infinity of the shrinking-core model is

$$S\,(\omega^g, \omega^s, T^*) = 9.02 \frac{3\gamma D_2 \varepsilon_s \omega^g \omega^s \rho_{rs}}{a^2} \qquad (5)$$

As can be seen from Figure 8.10, the way the oxygen consumption evolves in time using this form is not very much different from that using the shrinking-core model. Given that the overall oxidation rate is insensitive in many cases to the details of the intrinsic oxidation rate (Pantelis and Ritchie, 1991a), the above form has the attraction of simplicity.
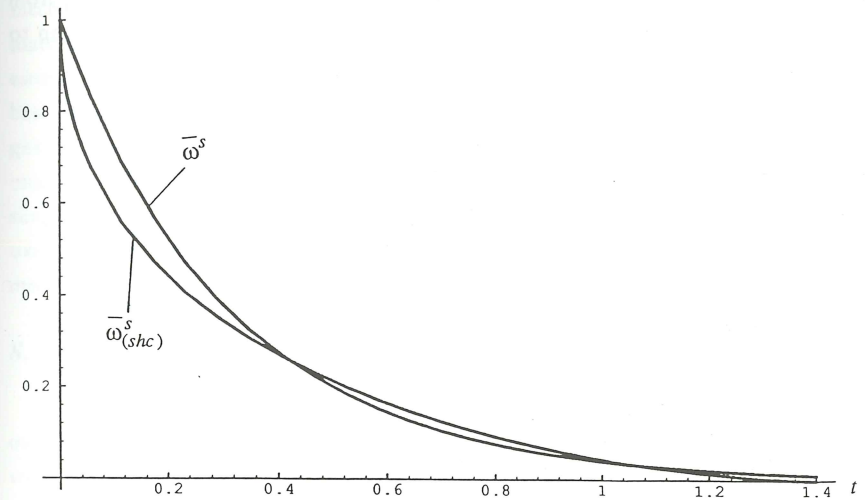

Figure 8.10. A comparison of the normalized sulfur mass fraction, ω^s of (5) with the normalized sulfur mass fraction, $\omega^s_{(shc)}$, of the shrinking-core form (3) (after Pantelis, 1993).

8.4.3. Typical Timescales in Gas Transport

Figure 8.11 defines and quantifies the timescales which appear naturally in the model equations describing gas and heat transport in waste-rock dumps. The same timescales will apply in other large pyritic dumps of waste material, such as tailings dams, but the physical form of the dump may preclude one or other of the transport

mechanisms. For example, convection is not likely to be a significant gas transport mechanism in a tailings dam because of the large ratio of area to height.

The longest timescale is that associated with diffusive transport of oxygen in the dump, and the shortest is that for oxidation of a single particle when the shrinking-core model is used to describe the intrinsic oxidation rate. Not surprisingly, Pantelis and Ritchie (1991a,b) have shown that, in a waste-rock dump in which gas transport controls the overall oxidation rate, a reduction in the time to oxidize a particle has little impact on the oxidation rate in the dump as a whole.

The timescale of 1.49 y for convection in Figure 8.11 is for a dump with an air permeability of 10^{-9} m^2, and becomes 14.9 y for an air permeability of 10^{-10} m^2 t. This is still much smaller than the 343-y timescale associated with diffusion. It is therefore noteworthy that Pantelis and Ritchie have shown that diffusive gas transport dominates over convective gas transport in a dump with an air permeability of 10^{-10} m^2 . One reason is that, initially, the only gas transport mechanism is diffusion. The temperature gradients that potentially drive convection are established on a diffusive timescale and are established in the toe of the dump batters. Temperature gradients resulting from ambient temperature changes are not large enough or deep enough in a dump to initiate convection.

Timescale for oxidation of pyrite in a particle

$$t_p = \frac{\epsilon \rho_{rs} a^2}{3 \gamma D_2 e_s C_o}$$

= 0.09 years for 4 mm diameter particle

(Time to completely oxidize a spherical particle is $t_p/2$)

Timescale associated with convection of gas through a heap with a competing chemical reaction

$$t_c = \frac{\epsilon \mu_a \rho_{rs} L}{K \rho_o^a g b T_o C_o}$$

= 1.49 years for 15 m high heap, K = 10^{-9} m^2, T_o = 30 °C

Timescale for diffusion of gas through heap with a competing chemical reaction

$$t_D = \frac{\epsilon \rho_{rs} L^2}{C_o D}$$

≈ 307 years for a 15 m high heap

Timescale for thermal diffusion in a heap

$$t_T = \frac{L^2}{\pi^2 \kappa}$$
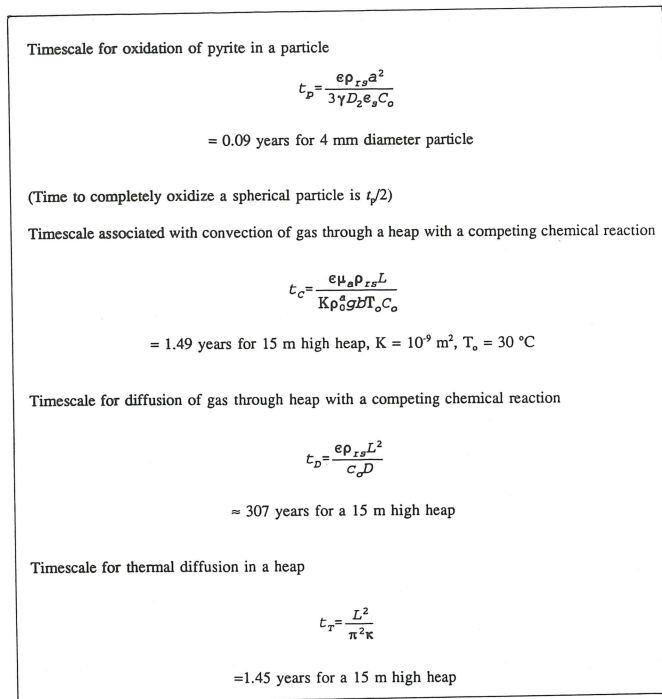
=1.45 years for a 15 m high heap

Figure 8.11. Characteristic timescales.

As long as gas specific-discharge rates are very small, heat transport is largely diffusional and the timescale to establish a new temperature distribution is that given in Figure 8.11. The L^2 dependence means that this characteristic timescale increases rapidly with increasing dump height. This long timescale to establish a new temperature distribution is another reason why diffusive gas transport dominates over convective gas transport in many waste-rock dumps. In biooxidation heaps, which are generally smaller than waste-rock dumps and in which every attempt is made to promote convective gas transport (Pantelis and Ritchie, 1993), temperature distributions are established quickly as heat transport by gas flow is significant. These points underscore the interactive nature of gas and heat transport in defining the oxidation rate in a waste-rock dump.

8.5. THE SPACE AND TIME DEPENDENCE OF THE OXIDATION RATE

Temperature and oxygen profiles can be analyzed both to extract the oxidation rate in a region of pyritic material and to determine the dominant gas-transport mechanisms. With this information and data on bulk physical properties of the dumped material, the primary pollution-production rate can be calculated; from this result an estimate can be made of the time dependence of pollution load in drainage from the base of the pyritic material. It is therefore useful to know what temperature and pore-gas oxygen-concentration profiles to expect for different forms of the intrinsic oxidation rate. The intent in the section below is to show the profiles expected for some simple forms of the intrinsic oxidation rate, and how the profiles change as the intrinsic oxidation rate changes. The profiles expected when convection is a significant transport mechanism, and the conditions under which convection occurs, will also be addressed.

8.5.1. The Simple Constant-rate Model (SCRM)

In the SCRM model the intrinsic oxidation rate is independent of pore-gas oxygen concentration and of the pyrite concentration unless these approach zero, whereupon it is assumed that the intrinsic oxidation rate tends to zero. Although this model may seem very simplistic, there is evidence (D.K. Gibson, 1992 private communication) that it applies to some pyritic material. It is also the form to which the intrinsic oxidation rate given by expression (4) tends when σ_1 and σ_2 are very small. Let us further assume that this intrinsic oxidation rate applies in a dump with the physical properties given in Table 8.3. Again for simplicity we assume that the dump was built sufficiently quickly that little or no pore-space oxygen was consumed during the construction phase and, further, that the moisture content of the dump at completion was the equilibrium one for the infiltration rate given. Neither of these two assumptions is crucial.

It is easy to show that if the equations are made dimensionless, $S = 2$, where

$$S = \frac{L^2 S^*}{DC_o} \qquad (6)$$

and

$$S^* = IOR \qquad (7)$$

is a critical value in the sense that, when $S < 2$, oxidation occurs throughout the pyritic wastes; when $S > 2$, oxidation is confined to a region within the wastes. When $S > 2$, oxidation is confined initially to a region $0 \le x \le x_1$ near the surface of the waste dump until all the pyrite is oxidized. Oxidation then moves to a second region $x_1 \le x \le x_2$ and is confined to that region until again all the pyrite in it is oxidized. This stepping process continues until the oxidation region encompasses the bottom of the wastes (assuming that these are not water-saturated). When the first region is fully oxidized, oxygen diffuses into the lower region and after some time a new concentration profile is established. The characteristic timescale for this is $L^2/(\pi^2 D)$ which, at about 0.15 years using the parameter values in Table 8.3, is much shorter than 170 years for the characteristic timescale of $(\varepsilon \rho_{rs})/S^*$ associated with oxidation of the pyrite. It is therefore legitimate to neglect initially the short time to establish the new profile and to treat the problem as pseudo steady state.

The points x_n are given by Gibson *et al.* (1994):

$$x_n = \sqrt{n} x_1 \qquad (8)$$

$$x_1 = \sqrt{\frac{2}{S}} \qquad (9)$$

Because the intrinsic oxidation rate is independent of oxygen concentration, the same rate applies in all regions, and hence the time to oxidize the pyrite in each region is the same.

The global oxidation rate, however, decreases with time because the regions to which oxidation is confined decreases with each step. At the time, t, oxidation is confined to the region:

$$x_n^* - x_{n-1}^* = (\sqrt{n} - \sqrt{n-1}) \sqrt{\frac{2C_o D}{S^*}} \qquad (10)$$

and the

$$GOR = \sqrt{2C_o D S^*} \, (\sqrt{n} - \sqrt{n-1}) =$$

$$\sqrt{2C_o D S^*} \left[\sqrt{\frac{S^* t^*}{\varepsilon \rho_{rs}} + 1} - \sqrt{\frac{S^* t^*}{\varepsilon \rho_{rs}}} \right] \qquad (11)$$

These points are illustrated in Figure 8.12.

As the ratio S^*/D increases, the global oxidation rate tends to a curve with a $t^{-1/2}$ dependence. As D does not vary by more than a factor of about 2 to 3 in unsaturated wastes (see Chapter 5), the main variable in the ratio S^*/D is the intrinsic oxidation rate. Assuming a dump height of 15 m and a diffusion coefficient in the wastes of 5×10^{-6} m^2 s^{-1}, then $S = 2$ for an intrinsic oxidation rate of 1.1×10^{-8} kg (O$_2$) m^{-3} s^{-1}. If the intrinsic oxidation rate is ten times greater and the diffusion coefficient remains the same, oxidation is confined to regions within the dump only about 1 m deep and the time dependence of the global oxidation rate is close to $t^{-1/2}$.
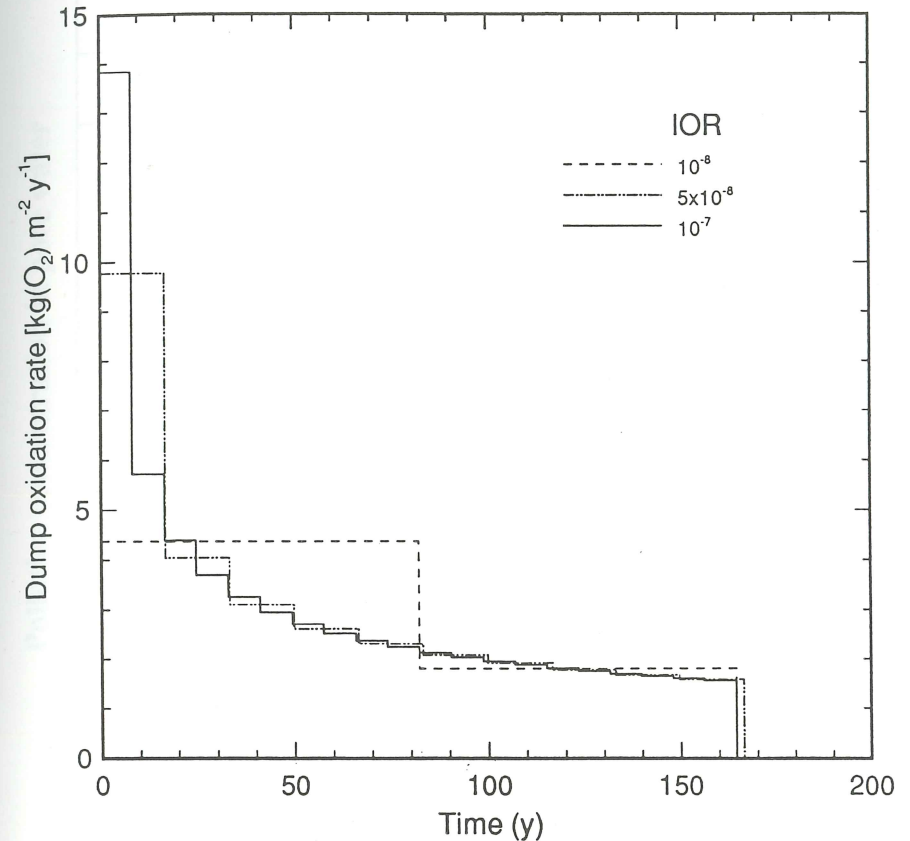

Figure 8.12. The overall oxidation rate (GOR) as a function of time for the simple constant-rate model for three values of the IOR, dump height 20 m, sulfur density 15 kg m^{-3} (after Gibson *et al.*, 1994).

The pore-gas oxygen concentration has the form shown in Figure 8.13a when $S > 2$, and is similar to that in Figure 8.13c. A more rigorous treatment, which includes the time dependence of the gas redistribution at the end of each step (Gibson *et al.*, 1994), confirms the utility of the pseudo-steady-state approach. The pollutant concentration is shown schematically in Figure 8.14a as a function of distance into the
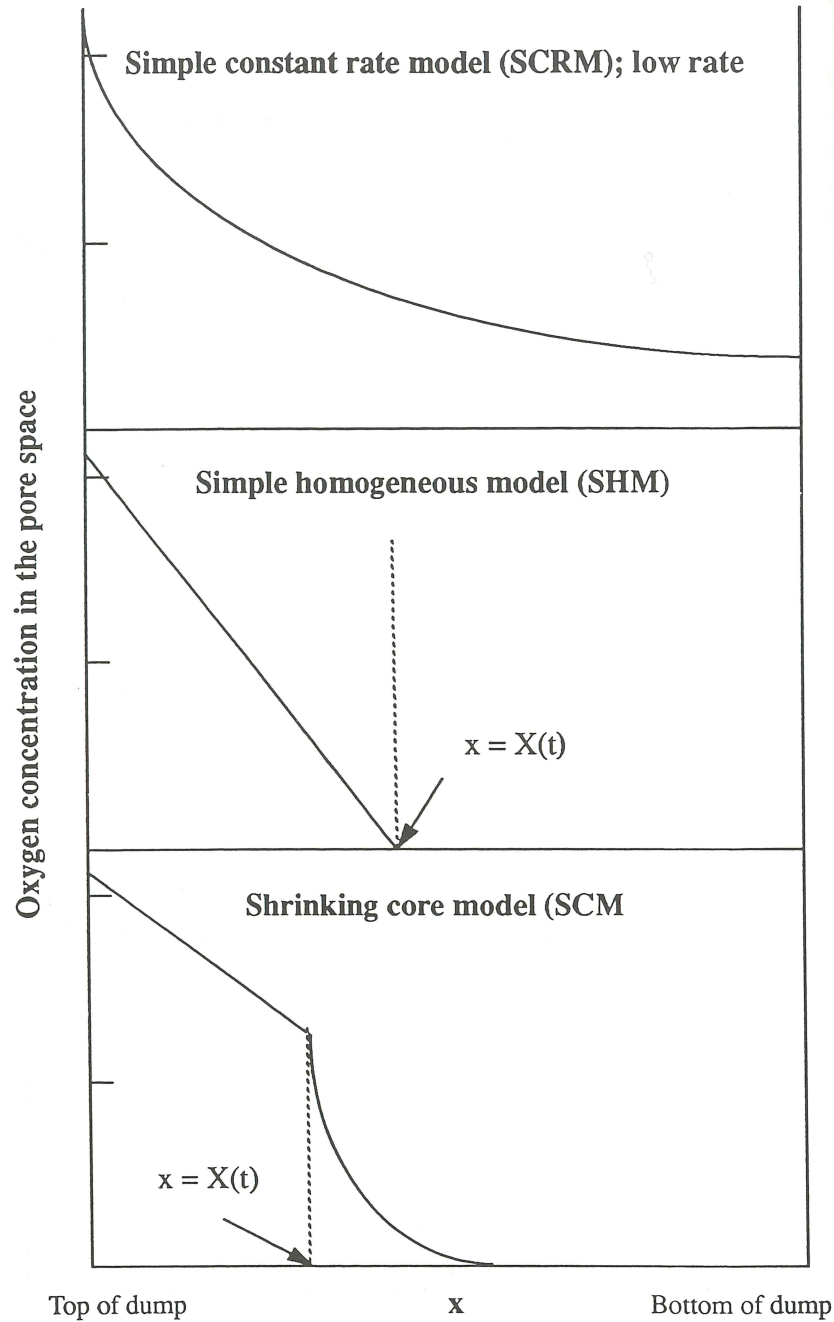
Figure 8.13. Oxygen-concentration profiles for different models of the intrinsic oxidation rate (IOR).
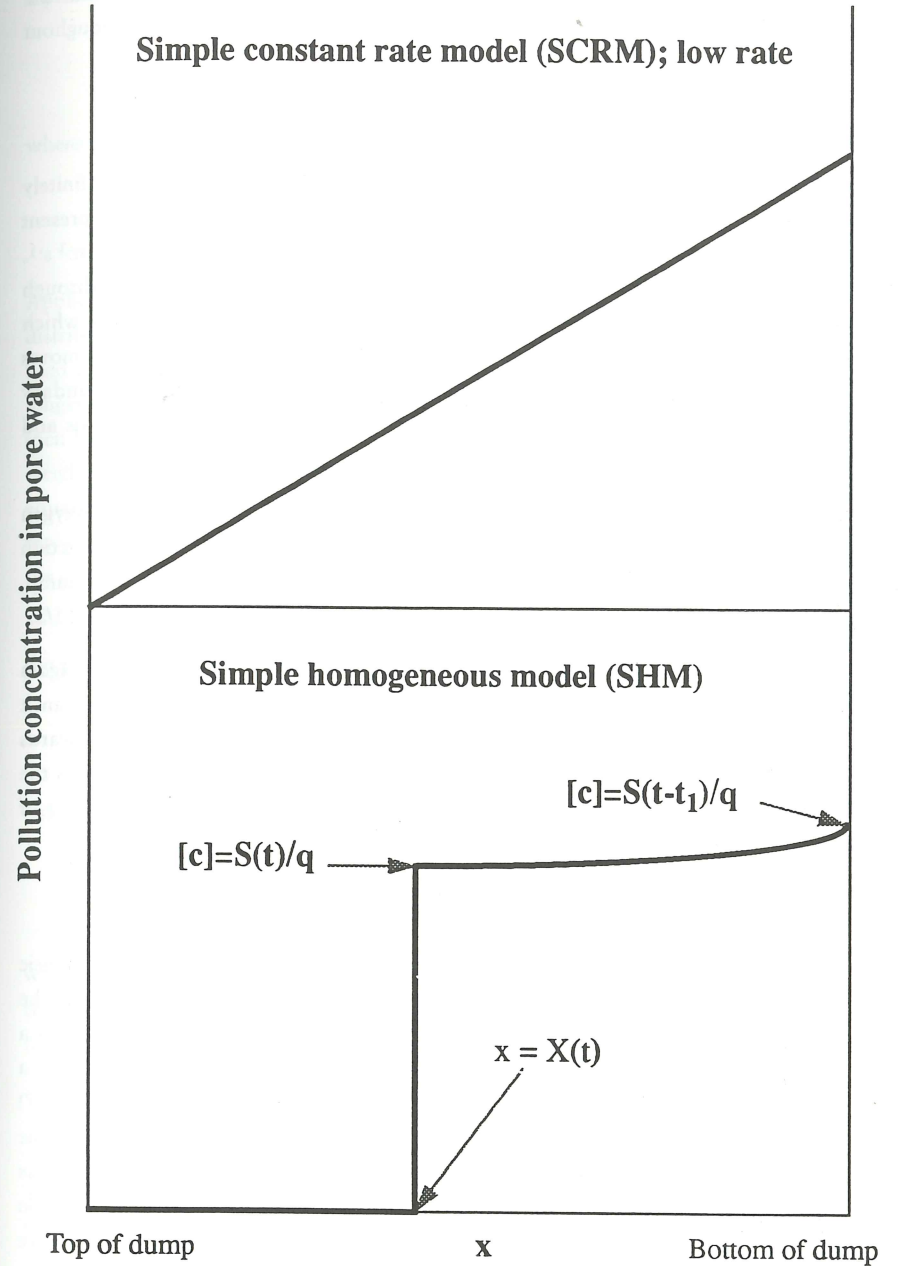

Figure 8.14. Sulfate concentrations in pore water for different models of IOR.

dump for the case where oxidation occurs throughout the dump. The assumption here is that a long enough time has elapsed that any transients associated with the transit time of pollutants through the dump can be neglected. It is also assumed that the pollutant concentrations remain below the solubility limit of the pollutant throughout the depth of the dump.

8.5.2. The Simple Homogeneous Model (SHM)

The SHM model is in effect the simple constant-rate model, but with an infinitely high oxidation rate for the waste material. It should be noted that, in the present context, an "infinitely high" intrinsic oxidation rate is only about 10^{-7} kg (O_2) m^{-3} s^{-1}. In this model it is assumed that the oxidizable material is uniformly distributed through the dump, and that the oxidation rate in the dump is limited by the rate at which oxygen can be supplied to an oxidation front which starts at the surface and moves into the dump. In mathematical terms the model is a classical moving-boundary problem (Crank, 1956), and its properties have been discussed elsewhere (Davis and Ritchie, 1986).

The oxygen concentration takes the form shown in Figure 8.13b, and the oxygen consumption rate in the dump is given by equation (1). The position of the reaction front is given by equation (2). When the reaction front reaches the base of the dump, all of the pyrite in the dump is oxidized; from equation (2), this occurs at time $t_d = 1/2$.

The pollutant concentration is shown schematically in Figure 8.14b, where again it is assumed that enough time has elapsed so that transients associated with the transit time through the dump can be neglected. The slight increase in concentration towards the base of the dump reflects the fact that the pollutant concentration here reflects the rate of pollutant generation at some earlier time which, given the $t^{-1/2}$ dependence of the oxidation rate, is higher at earlier times.

8.5.3. The Shrinking-core Model

As discussed above, the shrinking-core model has the attraction that the intrinsic oxidation rate decreases as the pore-gas oxygen concentration decreases and as the quantity of oxidizable material decreases. Intuitively, this is a property we seek in a realistic intrinsic oxidation rate. The use of such a model to describe oxidation in a waste-rock dump has been studied in some detail by Davis and Ritchie (1986, 1987) and Davis *et al.* (1986). The shrinking-core model gives rise to a moving front in the dump, above which there is no oxidation because all of the oxidizable material has been consumed. In practical terms there is another region below the oxidation region where the oxidation rate is negligibly small. The resulting oxygen concentrations have the form shown in Figure 8.13c.

The location of the upper front $x = X(t)$ in a dump composed of particles of just one size is given by the condition $R = 0$, where R is the position of the reaction front in a particle. This condition can be restated as

$$w\,(X,\,t\,) = \frac{1}{6k} \qquad (12)$$

where

$$w\,(x,\,t\,) = \int_0^t u\,(x,\,\tau)\,d\tau \qquad (13)$$

Application of this condition also allows the ready incorporation of a particle-size distribution into the intrinsic oxidation rate in a natural way because condition 12 is used to test whether or not a particle of a given size has been fully oxidized and no longer contributes to oxygen consumption at that point. The intrinsic oxidation rate then becomes an integral in which the integrand has the form of expression (3), with a weighting function to represent the particle-size distribution. In practice, as the set of equations has to be solved numerically (Davis and Ritchie, 1987), the integral is replaced by a sum; condition (12) is used to select those particle sizes to be included in the sum at a particular point in space and time.

The expression can also be used to quantify the time t_c during which a particle at the surface of the dump continues to oxidize. Because at the surface $w(x,t)$ is just t,

$$t_c = \frac{1}{6k} \qquad (14)$$

Another useful expression is

$$t = t_c + \frac{X^2}{2} + t_c\sqrt{\beta}X \tanh\sqrt{\beta}\,(1-x\,) \qquad (15)$$

which can be used to evaluate the position of the moving front $X(t)$, above which all of the pyritic material is oxidized. This expression can also be used to evaluate the time t_d to oxidize the whole heap. This takes the simple form

$$t_d = \frac{1}{2} + t_c \qquad (16)$$

This is just the time to oxidize completely the particle at the surface of the dump, t_c, together with the time for the moving front $X(t)$ to travel the full depth of the dump. As the particle size tends to zero, so does t_c, and expression (16) becomes identical to the result given by the simple homogeneous model.

Davis and Ritchie (1986) also showed that oxygen concentration in the region $X(t) \leq x \leq 1$ is approximated by

$$\bar{u}(x, t) = \frac{t_c \cosh\sqrt{\beta}\,(1-x)}{\left[t - \dfrac{X^2}{2}\right] \cosh\sqrt{\beta}\,(1-x)} \tag{17}$$

and the global oxidation rate by

$$S(t) = \frac{L\,\varepsilon\rho_{rs}}{\tau_4} \frac{1}{\sqrt{2t - t_c}} \tag{18}$$

The pore-gas oxygen concentration is shown schematically in Figure 8.13c. It is clear from the form of the global oxidation rate that, at long times, it takes on the $t^{-1/2}$ dependence of the simple homogeneous model. It also follows that, as the particle size tends to zero, the intrinsic oxidation rate of the shrinking-core model tends to that of the simple homogeneous model, t_c tends to zero, and the global oxidation rate has the same form as that of the simple homogeneous model.

In this sense the simple homogeneous model and the simple constant-rate model can be taken as useful extreme cases of the form taken by the intrinsic oxidation rate. It is also apparent from these three simple models that, unless the intrinsic oxidation rate is so low that much of the dump is involved in oxidation, the global oxidation rate tends to a $t^{-1/2}$ dependence after an initial transient. The length of this transient reflects details of the intrinsic oxidation rate, and stems from the way in which oxygen penetrates the surface regions of the dump. The implication is that, in a large mature dump, the global oxidation rate decreases as $t^{-1/2}$ and approaches the form given by equation (1). It is then largely independent of the details or magnitude of the intrinsic oxidation rate. It follows that the pollution load in drainage at the base of a dump, if averaged over, say, a year to remove fluctuation due to short-term fluctuations in infiltration rate, will have this same long-term time dependence. This is the reason why acid rock drainage is a long-term problem and why speeding up oxidation rates in a waste-rock dump is rarely a practical proposition.

8.5.4. Convection

As indicated above, the pollutant-generation rate in a large dump in which diffusion is the dominant gas transport process and in which the intrinsic oxidation rate is low, tends to decrease as $t^{-1/2}$ in the long term. The oxygen concentration decreases from the outer surface into the interior of the dump. The much shorter timescale associated with convective gas transport raises the spectre of high pollution-generation rates, but also opens the possibility of completely oxidizing the pyritic material in a dump in a time period short in comparison with the lifespan of a mining
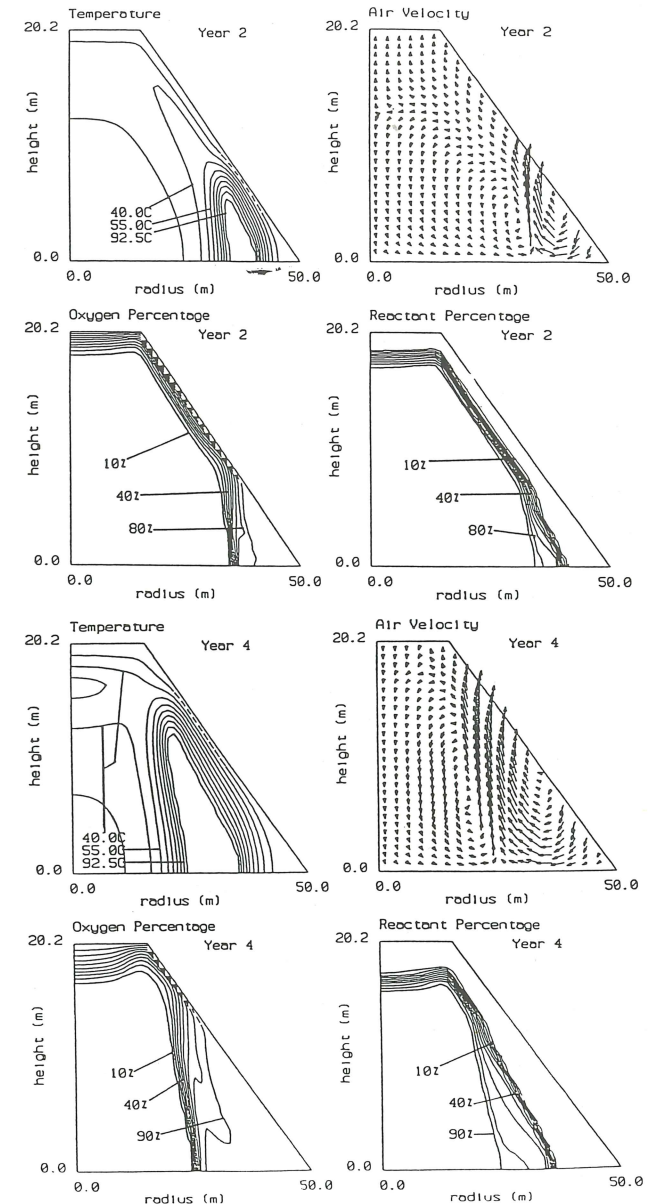

Figure 8.15. Profiles of temperature, gas velocity, fractional concentration of oxygen, and fractional concentration of remaining oxidizable material in a truncated cone-shaped heap at 2 and 4 years. The air permeability is $K = 10^{-9}$ m², the IOR is the shrinking-core model with $a = 0.005$ m, the maximum air velocity components are $|V_x|_{max} = 1.6 \times 10^{-5}$ m/s, $|V_z|_{max} = 6.3 \times 10^{-5}$ m/s at 2 years, and $|V_r|_{max} = 1.7 \times 10^{-5}$ m/s, $|V_z|_{max} = 7.8 \times 10^{-5}$ m/s at 4 years (after Pantelis and Ritchie, 1991b).

operation.

Cathles and his co-workers (1980) have modelled the effect of convection in copper heap-leach piles, and Pantelis and Ritchie (Bennett *et al.*, 1989; Pantelis and Ritchie, 1991a,b, 1992 1993) have modelled diffusion and convection in waste-rock dumps and biooxidation heaps in which the pyritic material has a relatively high intrinsic oxidation rate. The work of Pantelis and Ritchie indicates that oxidation in a newly built waste-rock dump proceeds initially by diffusion but, after some time, convection builds up in the toe of the dump batters. Convective transport of gas penetrates further into the dump as it ages. The evolution of the oxygen and temperature profiles is shown as a function of time for a typical dump in Figure 8.15.

8.5.5. Summary

The dependence of the global oxidation rate on such dump properties as the intrinsic oxidation rate, the air permeability, the gas diffusion coefficient, the infiltration rate, and the thermal conductivity is complex because the various transport processes are interactive and non-linear. Pantelis and Ritchie have shown that the following general principles apply to waste-rock dumps and biooxidation heaps:

- convection is not a significant gas transport mechanism in a dump where the air permeability is 10^{-10} m^2 or less (Pantelis and Ritchie, 1991a,b; Bennett *et al.*, 1989)

- convection is a significant gas transport mechanism in a dump in which the air permeability is 10^{-9} m^2 or more (Pantelis and Ritchie 1991a,b; Bennett *et al.*, (1989)

- convection is most effective in the batters of the dumps; diffusion dominates in the central regions of a dump (Pantelis and Ritchie, 1992)

- the global oxidation rate is very insensitive to increases in the intrinsic oxidation rate (Pantelis and Ritchie 1991a,b; Bennett *et al.*, 1989)

- the global oxidation rate is sensitive to irrigation rates in a dump with a high global oxidation rate (Pantelis and Ritchie 1991b)

It needs to be stressed that these are general principles, and the performance of a waste dump or biooxidation heap needs to be considered on a case-by-case basis. For example, allowing gas entry at the base of the dump and the possibility of forced aeration (Pantelis and Ritchie, 1993) removes the limitation set by diffusion and natural convection on gas transport rates in dumps that are closed to gas transport at the base. In such a situation the high global oxidation rate required can only be achieved at a high intrinsic oxidation rate for the heap material. The intrinsic oxidation rate sought in such cases is of the order of 10^{-6} kg(O$_2$)m^{-3}s^{-1}. Such high values of intrinsic oxidation rate can be achieved (Brierley, 1993).

8.6. FIELD MEASUREMENTS OF THE OXIDATION RATE

8.6.1. General Principles

It is evident from Sections 4 and 5 that the oxygen profile within a large waste-rock dump is pseudo steady state on a timescale of years, except in some special circumstances (see, for example, pronounced diurnal variations; Harries and Ritchie, 1985). If diffusive gas transport dominates over other forms of gas transport in some parts of the dump, and if the intrinsic oxidation rate is low as quantified in Section 5, then the oxygen profile is a reflection of the intrinsic oxidation rate. If, in addition, the variation within the dump can be taken as one-dimensional, as is usually so in large parts of a waste-rock dump, then the pore-gas oxygen concentration is described by the equation

$$\frac{\partial^2 u}{\partial x^2} = S(x) \qquad (19)$$

$$S(x) = \frac{L^2}{DC_o} S^*(x^*) \qquad (20)$$

where the variables S and x have been made dimensionless in an obvious way. The task is then, on the basis of measurement of the pore-gas oxygen concentration, to estimate the curvature of the oxygen-concentration profile at a point, and to evaluate the oxygen consumption at that point. It is worth remembering in conducting such an analysis that $\delta u / \delta x = 0$ at the point where the oxygen concentration goes to zero (Elliot and Ockenden, 1982) as a result of oxygen consumption in the dump when the intrinsic oxidation rate is of particular, but useful, form.

As in most waste-rock dumps the rate of heat transport by gas flow is generally small compared to the rate of heat transport by conduction, the direct effect of convective and advective gas flow on the temperature profiles is much less than on pore-gas oxygen profiles. Hence, if it is clear from the shape of the oxygen-concentration profile that gas transport mechanisms other than diffusion are important, then analysis of temperature profiles to extract the intrinsic oxidation rate may be more practical than analysis of oxygen profiles. In one dimension, the temperature within the dump is described by

$$\frac{\partial^2 T}{\partial x^2} = -\frac{\gamma DC_o}{T_o K_T} S(x) \qquad (21)$$

where again the variables have been made dimensionless. Again the task is to estimate the curvature of the temperature profile from the measured temperature distribution.

The temperature distribution in the waste material is a sum of the temperature distribution due to ambient temperatures and that due to heat sources in the wastes. This aspect is of particular significance near the surface of the wastes, where the temperature profile is commonly dominated by ambient temperatures. As the temperature changes that are due to ambient changes in surface temperature propagate into the dump, they are attenuated at a rate depending on their frequency. In principle, the temperature variation due to ambient changes in temperature is given by the expression (see Chapter 5 for more details)

$$T^*(x, t^*) = \sum_n u_n A_n(x) \cos(\omega_n t^* + \theta_n + \Psi_n(x) - \phi_n) \qquad (22)$$

In practice, the amplitudes of all of the components except those associated with the annual variation are small. Moreover, because the attenuation constant increases with increasing frequency, temperature variations caused by variations on the timescale of a month or less are small a meter or more from the surface. Hence, if temperature measurements are taken approximately monthly over a period of at least a year, the effect of changes in the ambient temperature can readily be taken into account in the data analysis. Similarly, the effect of heat transport by water infiltrating the dump is small and can be readily taken into account.

If convection is significant and it is important to extract the oxidation rate from the region of the dump where convection occurs, then one-dimensional analysis of the measured temperature profiles may not suffice. Because the heat source is proportional to the intrinsic oxidation rate, a simultaneous analysis of temperature and oxygen profiles yields the intrinsic oxidation rate. As such an approach requires an estimate of the curvature of the profiles in the two phases (horizontal as well as the vertical), a large grid of profiles would be required. Analysis of the data is most readily done by accessing a code that evaluates the two-dimensional temperature and oxygen profiles. Such a code is FIDHELM (Pantelis 1993), which solves the set of equations presented in Figure 8.9 and employs at the user's option one of the three forms of the intrinsic oxidation rate discussed in Section 4.2.

The point was made in Section 8.5 that if the intrinsic oxidation rate is much more than about 10^{-7} kg m^{-3} s^{-1} then, in those parts of the dump where diffusion dominates, the overall oxidation rate in the dump and its time dependence tend to that given by the simple homogeneous model. This requires knowledge only of the gas diffusion coefficient and concentration of oxidizable material. It follows that we do not need to measure the intrinsic oxidation rate with great precision; rather, we need to know it within limits in order to achieve the goal of defining an effective rehabilitation strategy. Furthermore, if sulfate is largely conserved within the dump, then the sulfate load from the dump is a measure of the integrated oxidation rate. The measured sulfate load can be used, together with temperature and oxygen concentrations, to indicate that the oxidation rate of the material in the dump is known with a precision sufficient to assess various rehabilitation options.

8.6.2. Estimation of the Oxidation Rate from Heat Sources

The Rum Jungle mine was a uranium-copper producer in the Northern Territory of Australia in the 1950s and 1960s. The ore was removed by an open-cut operation that left three large waste-rock dumps (White's, Dyson's, and Intermediate) when operations stopped in 1971 and the minesite was abandoned (Davy, 1975). The White's and Intermediate dumps have been instrumented (Harries and Ritchie, 1981; Daniel et al., 1982) to allow measurements of the temperature and oxygen concentrations through the dumps. Both dumps were about 20 to 25 m high; White's was the larger, with an area of about 27 ha compared to that of Intermediate's 7 ha.

The climate at the minesite is tropical, with an average of 80% of the mean annual rainfall of 1.5 m falling in the period December to March. The variation in the monthly mean daily temperature is small, varying only between 30 °C in November to 25 °C in July.

Figures 8.16 and 8.17 show typical temperature and pore-gas oxygen profiles measured in two of the dumps. These profiles changed very slowly over a period of some five years, with the most marked change being a slow decrease, about 1 °C y^{-1}, in the highest temperatures (Harries and Ritchie, 1983). It was clear from these profiles that gas transport in much of the dump was by diffusion from the surface, but that convection occurred in one large region of each of the dumps (Bennett et al., 1988). The temperature profiles were analyzed assuming one-dimensional heat transport to extract the heat-source distribution and hence the oxidation-rate distribution at a number of points in both dumps (Harries and Ritchie, 1981, 1987). The effect of the variable ambient temperature was accounted for, as was the effect of rainwater infiltrating the dump. The heat-source distributions are shown in Figure 8.18. Using a heat output of 1.29 J kg^{-1} released in the oxidation of pyrite, the corresponding values of intrinsic oxidation rate range from about 0.3 kg m^{-3} s^{-1} to 8.8×10^{-8} kg m^{-3} s^{-1}. The lower limit of detection of this technique under the experimental conditions in that situation was about 0.02×10^{-8} kg m^{-3} s^{-1}.

8.6.3. Estimation of Oxidation Rates from Oxygen-concentration Profiles

The Aitik minesite is in the north of Sweden, about 100 km north of the Arctic Circle. The mine is operated by Boliden Minerals AB and is Europe's largest copper mine. It is an open-cut operation producing about 14 million tonnes of waste rock a year. The waste-rock dumps have been constructed by end-dumping from trucks and flattening by bulldozers. The dumps are typically 35 m high and currently cover a total
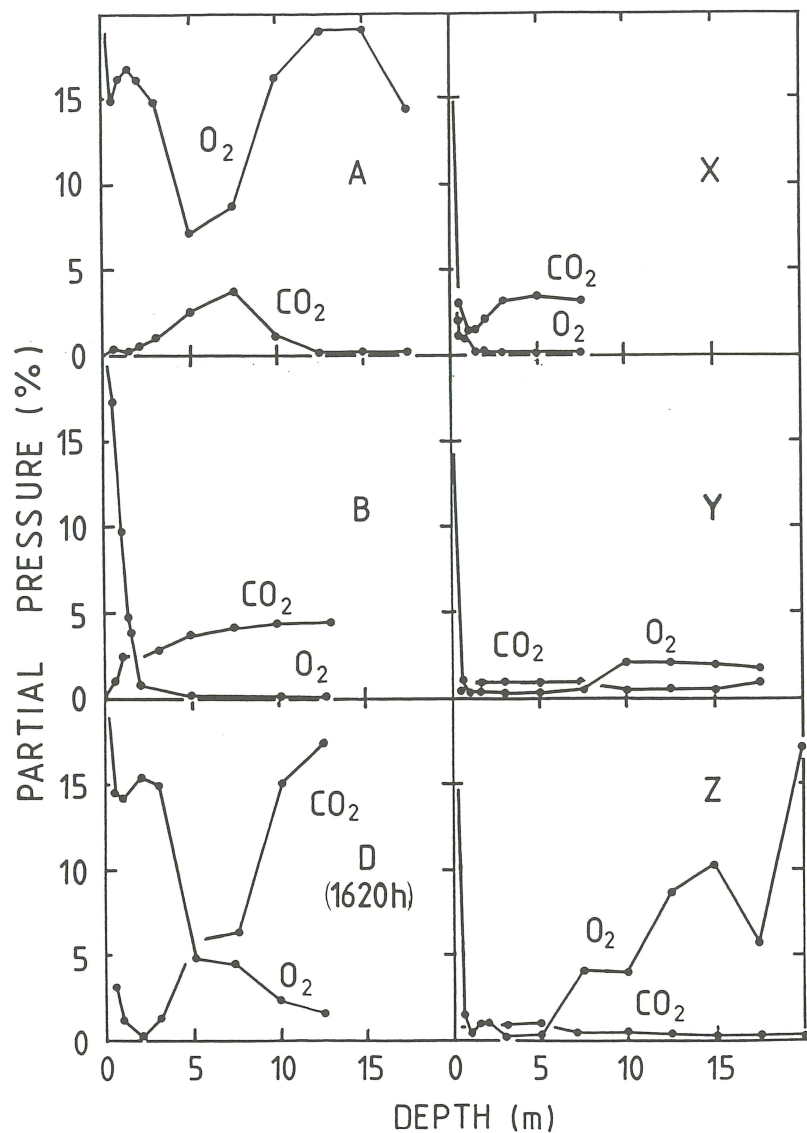
Figure 8.16. Oxygen and carbon dioxide concentrations as a function of depth in White's (locations A, B, D) and Intermediate (locations X, Y, Z) waste-rock dumps at the Rum Jungle minesite (after Harries and Ritchie, 1983).
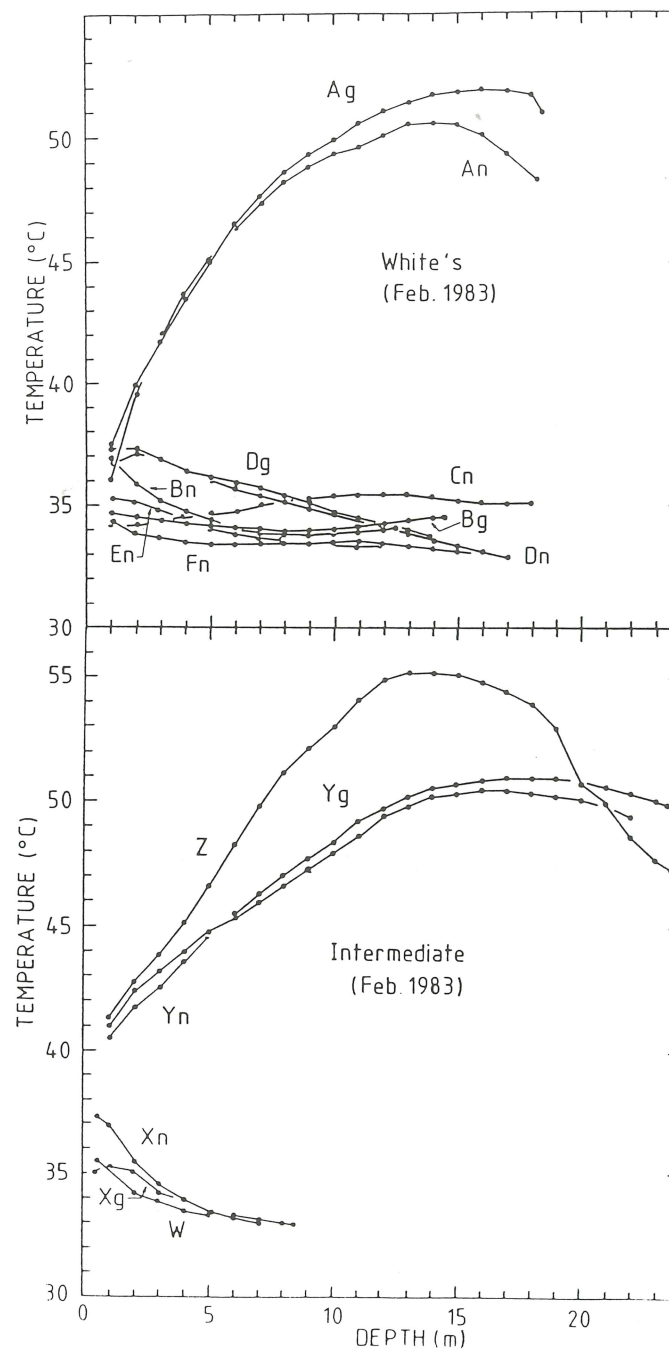

Figure 8.17. Temperature profiles in White's and Intermediate waste-rock dumps at the Rum Jungle minesite (after Harries and Ritchie, 1983).
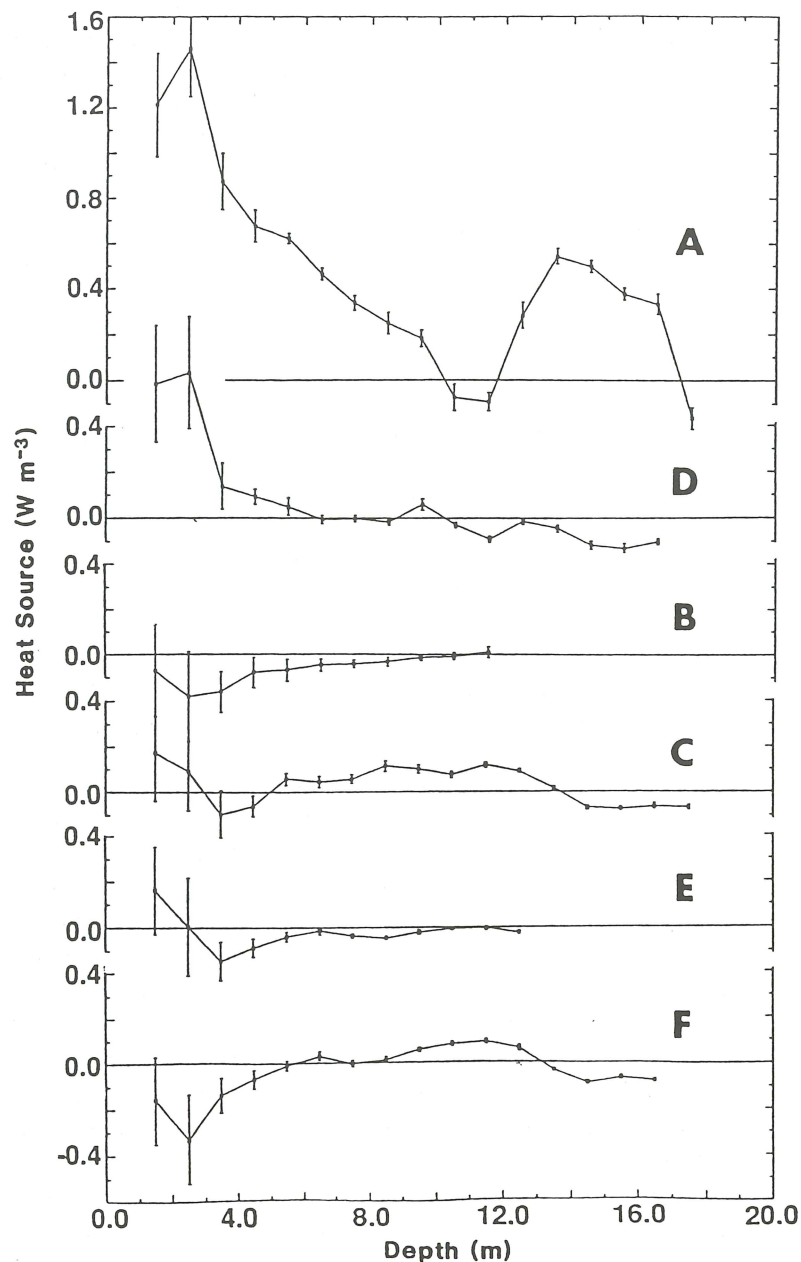
area of about 300 ha. The average annual temperature at the site is close to 0 °C, ranging from about 15 °C in July to about -15 °C in January. The average precipitation is 680 mm/yr, with a net infiltration into the waste rock of about 500 mm/yr (Axelsson et al., 1992). From about the middle of October to the middle of April, precipitation is mainly in the form of snow which melts over a period of a few weeks, usually in May.

Instrumentation was installed to allow measurement of temperature and pore-gas composition in a 1.5-ha portion of a waste-rock dump with an area of about 130 ha. Instrumentation to measure flow rates and pollutant concentrations was also installed in a cut-off drain that collected effluent from the dump. More details of the dump and the installations are given by Bennett et al. (1994).

Oxygen profiles in the region of the monitored dump fell into one of the following three categories:

1. Profiles where the oxygen concentration decreased significantly with increasing depth into the dump;

2. Profiles where the oxygen concentration decreased very slowly with increasing depth into the dump;

3. Profiles where the decrease in oxygen concentration was generally very small, but where there was a sharp fall followed by a sharp rise in the concentration over a distance of a few meters.

Examples of profiles for categories 1 and 3 are shown in Figure 8.19. Temperature profiles measured in one of the probe holes are shown in Figure 8.20. These profiles are typical of all temperature profiles measured in the portion of the monitored dump.

The shape of the oxygen-concentration profiles and the clear lack of any significant heating within the waste-rock dump indicate that, where the levels of oxygen are close to atmospheric, there is little oxygen consumption by the dump material, and where there is a significant gradient, diffusion is the dominant gas-transport mechanism. The oxygen profiles show a variability from month to month, even in those parts of the dump where it is clear from the oxygen-concentration profiles that oxygen is being consumed at the highest rate. Detailed analysis of these profiles (Bennett et al., 1994) show that some of this time dependence is seasonal and can be ascribed to a very small temperature dependence in the oxygen-consumption rate (about a 30% increase in the range 0—17 °C). Analysis of the oxygen-concentration profiles in the portion of the dump that had the highest oxygen-consumption rate yielded an intrinsic oxidation rate of about 1×10^{-8} kg m^{-3} for material comprising the top 9 m where the dump was about 15 m high. The data were consistent with the assumption that the intrinsic oxidation rate of this material was independent of oxygen concentration in the range 10 to 21% mole fraction.

Figure 8.18. Heat-source distribution calculated from temperature profiles measured in the period March 1979 to September 1983 at locations in White's waste-rock dump at the Rum Jungle minesite (after Harries and Ritchie, 1987).
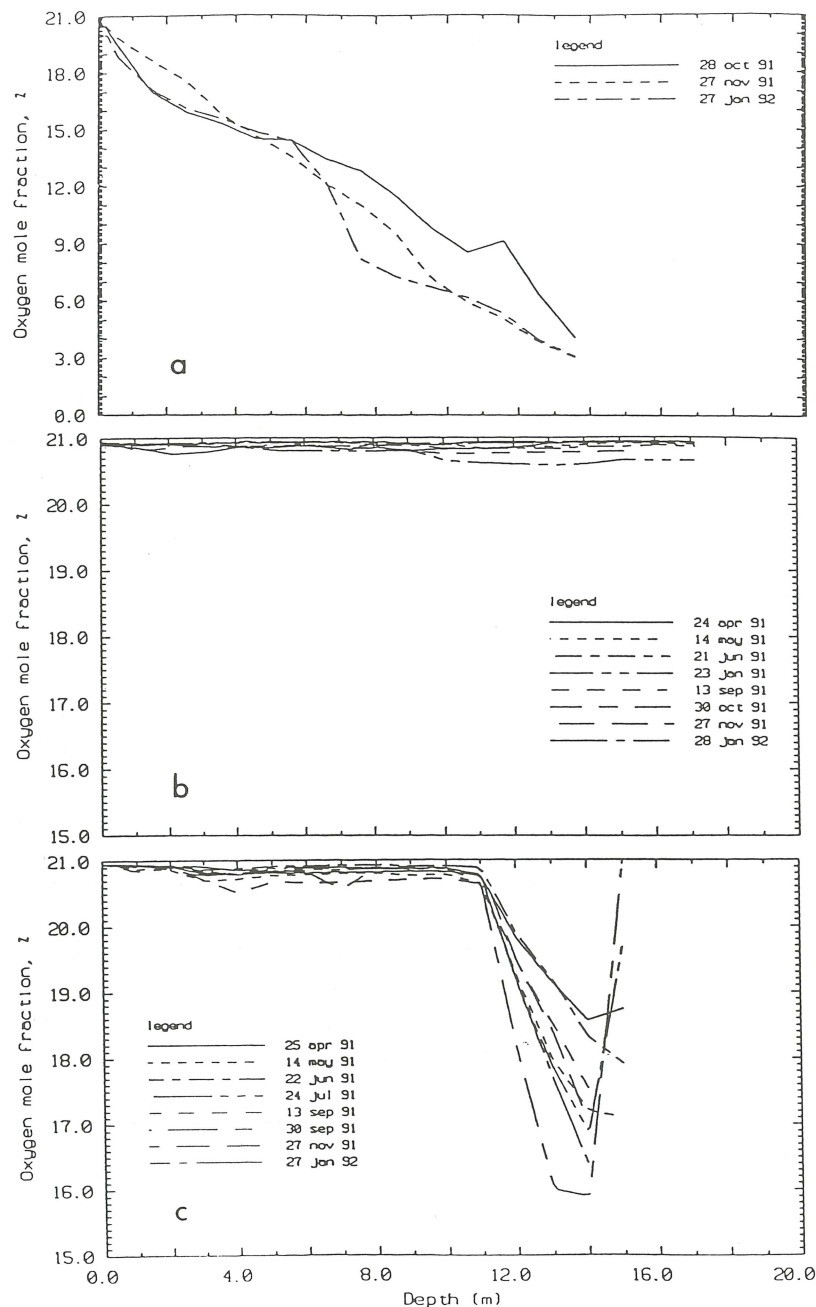
Figure 8.19.   Oxygen profiles in a waste-rock dump at the Aitik minesite, showing the three types of profiles: (a) a region of "high" IOR; (b) a region of very low IOR; (c) a pod of "high" IOR material in a region of very low IOR.
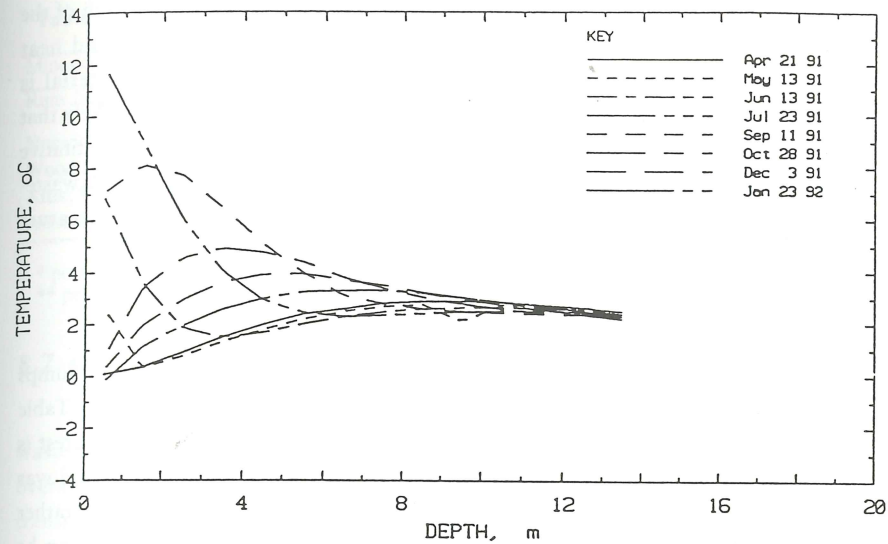
Figure 8.20.   Temperature profiles in a waste-rock dump at the Aitik minesite.

The oxygen flux into those regions of the dump where the intrinsic oxidation rate was high averaged 15×10^{-8} kg m^{-2} s^{-1}, compared with 0.25×10^{-8} kg m^{-2} s^{-1} in those regions where the intrinsic oxidation rate was generally low. The implication was that the contribution to the pollutant load in drainage from the latter regions was about 60 times less than that from regions of the dump containing material with an intrinsic oxidation rate of about 1×10^{-8} kg m^{-3} s^{-1}. The annual pollution load evaluated from flow rates and concentration levels in the cut-off drain were consistent with the assumption that some 20% of the dump material had the high intrinsic oxidation rate, and 80% had the vanishingly low intrinsic oxidation rate. It should be noted that the analysis of Section 5 shows that, when the intrinsic oxidation rate is low and gas transport is dominated by diffusion, the global oxidation rate increases with the square root of the intrinsic oxidation rate. This means that, if there are regions in the dump where the intrinsic oxidation rate is substantially higher than 1×10^{-8} kg m^{-3} s^{-1}, the conclusion that material having a high intrinsic oxidation rate comprises a comparatively small fraction of the total material in the dump will not be much changed.

8.6.4. Other Minesites

A comprehensive set of oxygen and temperature measurements has been made in some waste-rock dumps at the Heath Steele minesite in New Brunswick, Canada. The waste-rock dumps are comparatively small, with masses ranging from 3,250 tonnes to

235,700 tonnes, and heights from 3.4 m to 10.5 m. In such dumps, temperature changes due to ambient changes in temperature appear through the whole depth of the dump. To date, only qualitative conclusions have been reached on gas and heat transport in these dumps (Bell *et al.*, 1991). Oxidation of the dump material is apparent both from temperature and oxygen-concentration profiles. It seems likely that wind-driven advection is also a gas transport mechanism in these dumps. Quantitative analysis is expected to be available in 1994 (MEND Annual Report, 1992). A waste-rock dump at Mines Doyon in Quebec, Canada, has been instrumented to measure oxygen and temperature profiles (Gelinas *et al.*, 1992).

8.6.5. Data on Intrinsic Oxidation Rates

At this juncture there are little data on oxidation rates measured in large dumps of pyritic waste or from measurements that purport to be on run-of-mine wastes. Table 8.7 is a compilation of data on oxidation rates for run-of-mine material. Of interest is the last entry, which is for material in a large column in which the oxidation rate was measured directly (Bennett *et al.*, 1993a) from the rate of oxygen consumption rather than being inferred from the concentration of chemical species in drainage. It can be seen that this laboratory-measured rate is very much of the same order as that measured in the field for the dump material.

Another feature of the rates in Table 8.7 is that all are very much of the same order of magnitude and much lower than the "laboratory" measured rates in Table 8.1. There are two points to emphasize. First, the magnitude of the oxidation rates listed in Table 8.7 indicates that the intrinsic oxidation rate will be a large determinant in the early (years to tens of years) time dependence of the pollution load from the waste-rock dump (Gibson *et al.*, 1994, and Chapter 5). Second, the scaling-up of laboratory-measured intrinsic oxidation rates to those appropriate to run-of-mine waste rock must incorporate factors that account for the 2 orders of magnitude difference between the two types of results. Given the magnitude of the difference, and given that it is only if the intrinsic oxidation rate is less than about 1×10^{-7} kg m^{-3} s^{-1} that we need to know it with any precision, it may in practice be more cost-effective to measure the intrinsic oxidation rate directly in run-of-mine material.

It must be stressed that the rates listed in Table 8.7 cannot be typical of all bulk pyritic material. If they were, then it would be impossible to achieve the overall oxidation rates required to pre-treat some refractory gold ores in biooxidation heaps. That such treatment is indeed practical has been demonstrated by Brierley (1993). A technique to overcome the limitations in the rate of oxygen supply in such heaps has been quantified by Pantelis and Ritchie (1993).

Table 8.7. Measured intrinsic oxidation rates

Minesite	Entity	Reference	kg(O$_2$)m^{-3}s^{-1}
Rum Jungle, Australia	waste-rock dump	Harries & Ritchie (1981)	$(0.3 \text{ to } 8.8) \times 10^{-8}$
Norwich Park, Australia	coal rejects	*	$(0.3 \text{ to } 2.2) \times 10^{-8}$
Woodlawn, Australia	waste-rock dump	**	$(0.2 \text{ to } 2.7) \times 10^{-8}$
Aitik, Sweden	waste-rock dump	Bennett et al. (1993)	$(0.3 \text{ to } 4.3) \times 10^{-8}$
Aitik, Sweden	large columns	Bennett et al. (1993	1.4×10^{-8}

* personal communication from J.W. Bennett and Y. Tan, 1993
** personal communication from Y. Tan, 1993

8.7. CONCLUSIONS

The intrinsic oxidation rate defines the primary pollutant-production rate in a waste-rock dump. If the rate is high, and high is about 1×10^{-7} kg m^{-3} s^{-1}, then the overall oxidation rate is determined predominantly by the rate at which oxygen can be transported to oxidation sites within the waste-rock dump. If the rate is less than about 10^{-7}, then relatively large regions of the dump will be involved in oxidation, and the magnitude of the intrinsic oxidation rate will be a major control on the early time (years to tens of years) behavior of the pollution load from the dump.

Measurements in waste-rock dumps have shown that gas transport by diffusion is observed in many dumps, and that gas transport by convection is observed in some. Advective gas transport generated by, for example, wind blowing over a waste-rock dump, is a possible mechanism but has not been observed quantitatively. Convective gas transport is not likely to be significant in a dump unless the air permeability of the dump material is greater than about 10^{-9} m^2. Convection, if it occurs, starts in the batters of the dump and penetrates into the dump from there. In a large dump, oxidation is generally dominated by diffusive transport in the central regions of the dump.

Oxygen and temperature profiles reflect the oxidation rate and gas transport mechanisms in a dump. Analysis of measured profiles has been used to evaluate the intrinsic oxidation rate of deposited waste-rock dump material. The measurements yield values ranging from <0.3 to about 9.0×10^{-8} kg m^{-3} s^{-1}. These are low compared to values from measurements of pyritic oxidation rates in the laboratory, but are certainly large enough to be environmentally significant. Such is the large difference between the intrinsic oxidation rate derived from field measurements and those from laboratory measurements on crushed samples that there must be some doubt that all of the factors which need to be applied to crushed samples to scale up to run-of-mine material can be taken into account adequately. This is particularly so if scaling up yields values greater than about 10^{-7} kg m^{-3} s^{-1}, as then there is no need to know the

intrinsic oxidation rate with any precision because, in most waste-rock dumps, gas transport rates then control the primary pollution-production rates. Such is not the case when steps are taken, such as in biooxidation heaps, to ensure that gas transport rates are not rate-limiting. Such steps include ensuring that the air permeability is high, or constructing the heap to ensure that the bottom of the heap is open to gas flow.

Oxygen and temperature profiles in pyritic wastes are easily measured with inexpensive instrumentation once an appropriately constructed probe hole has been installed. As both these parameters are closely related to the pyrite oxidation rate, which is the primary pollutant-generation mechanism, they provide a direct and rapid indicator of the effectiveness of measures adopted to reduce the oxidation rate in pyritic mine-wastes. In this sense, monitoring these parameters provides more timely and more easily interpreted information on the effectiveness of rehabilitation, both in the short and in the long term, than does monitoring of drainage-water quality.

8.8. ACKNOWLEDGEMENTS

8.9. NOMENCLATURE

$T^* = $ temperature (°C)

$T_o = $ some characteristic temperature for normalization

$T = $ T^*/T_o dimensionless temperature

$x^* = $ spatial variable (m)

$L = $ height of waste-rock dump (m)

$x = $ x^*/L dimensionless spatial variable

$S^* = $ intrinsic oxidation rate (kg (O_2)m^{-3}s^{-1})

$S_S = $ oxidation rate of oxidizable material (kg (O_2)m^{-3}s^{-1})

$C_o = $ concentration of oxygen in air (0.265 kg m^{-3})

$c_w = $ specific heat of water (4.18 x 10^3 m^{2}s^{-2}K^{-1})

$D = $ oxygen bulk diffusion coefficient of dump (m^{2}s^{-1})

$S = $ $(L^2S^*)/C_oD$ = dimensionless intrinsic oxidation rate

$\kappa = $ bulk thermal diffusivity of dump (m^{2}s^{-1})

$\rho_s = $ bulk density of dump (kg m^{-3})

$\delta = $ heat released per mass of reactant oxidized (2.25 x 10^{7}J kg^{-1})

$\varepsilon = $ mass of oxygen used per mass of reactant in oxidation reaction (1.75)

$c_s = $ bulk specific heat of dump (886 m^{2}s^{-1}K^{-1})

$Q_w = $ infiltration rate (ms^{-1})

$b = $ thermal coefficient of expansion of air (3.4 x 10^{-3})

$D_2 = $ diffusion of oxygen in solid (m^{2}s^{-1})

$\rho_{a_0} = $ density of air at t_0

$\rho_\alpha = $ bulk density of α phase; g = gas, w = water, s =solid

$\rho^\alpha = $ intrinsic density of α phase

$\rho_\alpha = $ $\varepsilon_\alpha\rho^\alpha$

$\rho_{rs} = $ initial bulk density of reactant (kg m^{-3})

$\varepsilon_\alpha = $ volume fraction of α phase; g = gas, w = water, s =solid

$u(x,t) = $ **dimensionless oxygen concentration**

$u(x,t) = $ **expression for $u(x,t)$ corresponding to ($w(x,t)$)**

$\omega^g = $ mass fraction of oxygen in gas phase

$\omega^s = $ mass fraction of oxidizable material in solid phase

$w(x,t) = $ defined by equation (13)

$w(x,t) = $ **approximate solution for $w(x,t)$**

$\gamma = $ a proportionality constant encompassing both Henry's Law and the Gas Law (0.03)

$X^*(t^*) = $ position of planar moving front within dump (m)

$X = $ X^*/L = dimensionless position of planar moving front

$\beta = $ $6k$

$\tau_3 = $ $a^2\varepsilon \, \rho_{rs}/(\gamma\varepsilon_s C_o)$

$\tau_4 = $ $L^2\varepsilon \, \rho_{rs}/(DC_o)$

$t^* = $ time variable (s)

$t = $ t^*/τ_4 = dimensionless time variable

$k = $ $1/k_2$

$k_2 = $ τ_3/τ_4

$K = $ intrinsic air permeability of the dump (m^2)

$k_{rg}(\varepsilon_g) = $ relative air permeability of the dump; *in-situ* measurement of air permeability yields the product $Kk_{rg}(\varepsilon_g)$

$K_T = $ bulk thermal conductivity of the dump (W m^{-1} K^{-1})

$K_s = $ saturated hydraulic conductivity of the dump (ms^{-1} or md^{-1})

$a = $ radius of a particle (m)

$t_c = $ time for the particle at the surface to oxidize completely (s)

$t_d = $ time for the dump to oxidize completely (s)

$t_p = $ timescale for oxidation of a particle (s)

$t_C = $ timescale for convection of a gas through a dump (s)

$t_D = $ timescale for diffusion of a gas through a dump (s)

$t_T = $ timescale for thermal diffusion in a dump (s)